Predicting population dynamics from the properties of individuals: a cross-level test of Dynamic Energy Budget theory

Benjamin Martin[1*], Tjalling Jager[2], Roger M. Nisbet[3], Thomas G. Preuss[4], Volker Grimm[1,5]

[1] Helmholtz Centre for Environmental Research – UFZ, Department of Ecological Modelling 04318 Leipzig, Germany benjamin.martin@ufz.de, volker.grimm@ufz.de

[2] Vrije Universiteit Amsterdam, FALW/Department of Theoretical Biology, De Boelelaan 1085 NL-1081 HV Amsterdam, The Netherlands tjalling@bio.vu.nl

[3] University of California, Santa Barbara, Department of Ecology, Evolution, and Marine Biology, Santa Barbara, CA 93106-9620 nisbet@lifesci.ucsb.edu

[4] RWTH Aachen University, Institute for Environmental Research, Worringerweg 1, 52074 Aachen, Germany thomas.preuss@bio5.rwth-aachen.de

[5] University of Potsdam, Institute for Biochemistry and Biology, Maulbeerallee 214469 Potsdam, Germany

Key words: population dynamics, dynamic energy budget theory, bioenergetics, individual-based model

Type of submission: Article

Elements of the manuscript that will appear in the expanded online edition by title:

1. Appendix 1. Model parameterization
2. Appendix 2. Model Description (ODD)
3. Appendix 3. Supplementary figures
4. Netlogo model file

Abstract

Individual-based models (IBMs) are increasingly used to link the dynamics of individuals to higher levels of biological organization. Still, many IBMs are data hungry, species specific, and time consuming to develop and analyze. Much of these issues would be resolved by using general theories of individual dynamics as the basis for IBMs. While such theories have frequently been examined at the individual level, few cross-level tests exist which also try to predict population dynamics. Here we perform a cross-level test of DEB theory by parameterizing an individual-based model using individual-level data of the water flea, *Daphnia magna*, and comparing the emerging population dynamics to independent data from population experiments. We found that DEB theory successfully predicted population growth rates and peak densities, but failed to capture the decline phase. Increased food-dependent mortality of juveniles was needed to capture the population dynamics after the initial population peak. The resulting model then predicted, without further calibration, characteristic switches between small- and large-amplitude cycles, which were observed for Daphnia. We conclude that cross-level tests help detecting gaps in current individual-level theories and ultimately will lead to theory development and the establishment of a generic basis for individual-based models and ecology.

Introduction

Individual-based ecology (IBE) is a growing field. The general goal in IBE is to predict dynamics at higher levels of biological organization, for example population size, spatial distribution, or community structure, from an understanding of how individuals behave and interact with each other and their environment (Grimm and Railsback 2005). A major tool in IBE are individual-based models (IBM). They are used when one or more of the following three aspects are considered essential: differences among individuals, local interactions, and adaptive behavior (DeAngelis and Mooij 2005, Railsback and Grimm 2012).

However, a well-known drawback of IBMs is that they can be quite complex and data-hungry. Consequently, they often are designed for specific species where sufficient data exist. Model designs are then tied to these species and are thus more or less ad hoc. This makes model development and analyses inefficient because each model has its own set of assumptions. Moreover, different models are hard to relate to each other so that general insights can be hard to distill from both individual IBMs and IBMs in general (Grimm 1999, Grimm et al. 1999).

In contrast to this species-specific approach, some theoretical approaches attempt to deduce the diversity among organisms and ecological systems from generic models of individual-level processes, for example Dynamic Energy Budget (DEB) theory or the Ontogenetic Growth Model based on Metabolic Scaling Theory (Hou et al. 2008). These approaches are based on first principles of bioenergetics and thus focus on common and species-independent aspects of organisms and their performance. They apply the same generic model structure for all species and use variation in parameter values to explain differences in life-history patterns among species.

Such standardized, generic models hold great potential for advancing the field of IBE (Berger et al. 2002). First, they make model development and communication more efficient. This is important both for theoretical and applied models. Instead of designing models from scratch, standard designs can be used which do not need to be justified in detail, because they have been tested and used before. Second, they facilitate comparing models addressing different species and systems. Differences in model behaviour can be more easily ascribed to differences in species-specific traits or system-specific controls, whereas without standard submodels they could be ascribed to virtually any detail of the submodels' structure. Conversely, when the same model structure is used to model different species we can understand the differences in population level output as a function of differences in individual-level parameters.

Despite the great potential of generic individual-level models as the foundation for IBMs, their ability to accurately capture the dynamics of higher levels of biological organization remains largely untested. Here we focus on performing a cross-level test for one general theory, Kooijman's Dynamic Energy Budget theory (hereafter referred to as DEB) (Kooijman 2010, Sousa et al. 2010). DEB is a general theory which describes life history traits over time over a range of environmental conditions. DEB theory has been used to model individual level processes for a wide range of animal species, e.g. mollusks (Ross and Nisbet 1990; van Haren and Kooijman 1993; Saraiva *et al.* 2011), zooplankton (Nisbet *et al.* 2010), fish (Pecquerie *et al.* 2009; Pecquerie *et al.* 2011)), and to model population level processes for microorganisms (e.g bacteria, Kooi and Kooijman 1994; Hanegraaf and Muller 2001) and for phytoplankton (Muller 2011). Yet, a primary motivation of the development of DEB theory was to explain population dynamics in terms of individual life-history traits, i.e. to obtain unified theory across levels of biological organization (Nisbet et al. 2000). Surprisingly, however, so far tests of DEB theory that link individual and population process have been sparse and of limited scope (literature reviewed by Nisbet et al., 2010) or have focused on modeling equilibria or population growth rates, e.g. de Roos (2008).

So far, tests of DEB theory at the population level have been limited to situations where differences among individuals could be modeled with simple assumptions that justified using ordinary differential equations at the population level (e.g. Nisbet et al. 2000, Kooijman 2010, chapter 9). However, for many populations size-dependent relationships can be important, for example for metabolic allometric scaling (Woodward *et al.* 2010), foraging theory (Gergs and Ratte 2009; Woodward et al. 2010) as well as for uptake and sensitivity to toxicants (Hendriks 1995; Preuss *et al.* 2008). In these cases, an approach is needed that can keep track of differences between individuals, i.e. individual-based models.

Still, there are few direct quantitative tests of DEB at the population level that take advantage of the full flexibility of individual-based models. Such tests are needed, however, to explore the potential of DEB theory, or other generic theories, for predicting population dynamics (Grimm and Railsback 2005). The task is not to just test a theory, but to see how well it works, where it fails, and how it can be improved. Ecological systems are characterized by cross-level interactions, so that observations at lower levels can be used to infer mechanisms at higher levels, and vice versa (Grimm et al. 2005, Grimm and Railsback 2012). Testing DEB theory at the population level thus could provide hints at structural aspects of the theory that need reconsidering or further research. Moreover, such tests could show which aspects of the theory really matter at the population level, offering opportunities for simplification.

We here develop an IBM for a cross-level test of DEB theory to explore its potential to predict population dynamics. For implementing this IBM, we use the software tool DEB-IBM (Martin et al. 2012) which is a generic IBM based on individuals performing according to DEB theory. As a model system, we use laboratory populations of *Daphnia magna*, for which we collected independent data sets on individual performance and population dynamics under different environmental conditions. We first use individual-level data to parameterize a model of individuals that is based on DEB theory. Then, we use these DEB individuals to simulate population dynamics and compare them to results from independent population experiments.

We also test possible simplifications of the original DEB model as well as modifications that increase its predictive power. Finally, we test whether the resulting population model is able to reproduce, without any further calibration, additional qualitative patterns, for example the characteristic occurrence of both small- and large-amplitude cycles which has been observed under certain resource conditions.

Methods

The model

A detailed, comprehensive model description, following the ODD (Overview, Design concepts, Details) protocol for describing individual- and agent-based models (Grimm et al. 2006, 2010) is given in the Supplementary Material, as well as the source code of the model's implementation in NetLogo (Wilensky 1999). Here we briefly describe the DEB model representing the individuals' life histories, the model's schedule, and species-specific submodels of processes which are not fully covered by the "standard" DEB model (Sousa et al. 2010).

In the standard DEB model individuals are primarily characterized by four state variables (there are two additional state variables to characterize the ageing process [see below and supplementary material]): structural length, L, which determines actual size, feeding rates, and maintenance costs; scaled reserves, U_E, which serve as an intermediate storage of energy between feeding and mobilization processes; scaled maturity, U_H, a continuous state variable which regulates transitions between the three development stages (embryo, juvenile, adult) at fixed maturity levels; and scaled buffer U_R, which is an energy buffer of mature individuals for reproduction; this energy in converted into offspring during reproductive events.

Four differential equations specify how these state variables change, depending on their current values and the environmental conditions. We implemented a discretized version of the differential equations, using the Euler method. Each timestep, individuals forage and assimilated energy (rate S_A) first enters a reserve compartment (U_E), from which energy is mobilized (rate S_C) to fuel all other processes:

$$\frac{d}{dt}U_E = \left(S_A - S_C\right)$$

The scaled assimilation flux, S_A, is equal to the product of the scaled functional response, *f*, and the squared length of the individual $S_A = fL^2$, where *f* is given by the Holling type 2 functional response $\frac{X}{K+X}$, with *X* the density of the food and *K* the half-saturation coefficient. The mobilization flux, S_C, is given by:

$$S_C = L^2 \frac{ge}{g+e}\left(1 + \frac{L\dot{k}_M}{\dot{v}}\right) \text{ where } e = \dot{v}\frac{U_E}{L^3}$$

The derivation of this reserve dynamics implies that at constant food densities, animals will follow von Bertalanffy growth, and the scaled reserve density (*e*), the ratio of reserves to structure relative to the maximum reserve to structure ratio, will be constant. In constant food conditions $e = f$; if food level changes, *f* changes, and *e* will approach the new *f* (see Kooijman (2010) for the derivation of the reserve dynamics).

A portion (κ) of the mobilized energy is used to maintain current somatic structure and to synthesize new somatic mass.

$$\frac{d}{dt}L = \frac{1}{3}\left(\frac{\dot{v}}{gL^2}S_C - \dot{k}_M L\right)$$

The remaining proportion (1-κ) is allocated to maturation and reproduction. Before an animal has reached puberty, the proportion (1-κ) is allocated towards the maturity state variable.

$$\frac{d}{dt}U_H = (1-\kappa)S_C - \dot{k}_j U_H \text{ when } U_H < U_H^p$$

When an individual has reached puberty, energy from the maturity flux is diverted into a reproduction buffer, U_R, from which embryos are created.

$$\frac{d}{dt}U_R = (1-\kappa)S_C - \dot{k}_J U_H^p \text{ when } U_H \geq U_H^p$$

The *Daphnia* population dynamics are linked to the prey conditions as their feeding depletes the prey density. The amount of prey consumed is given by the summation the product of the scaled assimilation rate (S_A) and the maximum surface area specific ingestion rate ($\dot{J}_{XAm}$) of all *Daphnia* in the population (n)

$$\frac{dX}{dt} = -\sum_i^n \left(S_A \{\dot{J}_{XAm}\}\right)$$

Additionally, DEB theory has a submodel to handling the aging process, which contains two additional state variables and two parameters. Individuals accumulate damage inducing compounds ($\ddot{q}$) that in turn produce damage ($\dot{h}$; van Leeuwen et al. 2010), with the probability of dying due to ageing being proportional to the amount of damage individuals have accumulated (see ODD in supplementary material for full specification).

DEB theory makes no assumptions of how the reproduction buffer is converted into offspring because too many different strategies driving these processes exist. We therefore added that *Daphnia* reproduce in clutches, where energy allocated to embryos is accumulated over one molt (here assumed to have a fixed value, approximately every 2.8 days, throughout the life cycle). The embryos develop during the next molt, and hatch at the end of that molting period. Furthermore, we had to deal with the submodel for starvation. Within DEB theory, there are several proposed ways to include mortality via starvation (Kooijman 2010). In general, starvation occurs when the energy mobilized from the reserves and allocated to the soma is not sufficient to pay somatic maintenance costs. Variations of this starvation sub-model assume animals can redirect energy from the (1-κ) normally allocated to maturity (juveniles) or reproduction (adults) (Kooijman 2010). Our analysis of this set of starvation submodels revealed starvation times far too short (< 1 day), and thus were ruled out. This point was previously noted for *Daphnia pulex* (McCauley et al. 1990).

We selected a second type of starvation submodel for our simulations, which assumes that when there is not enough energy to pay somatic maintenance costs, individuals can "burn" structure to pay these costs ("shrinking"). *Daphnia* can survive extended periods of starvation, where their body mass can fall to 30-50% of their previous maximum body mass (Perrin et al. 1990; Bradley et al. 1991; Cluvers et al. 1997; Vanoverbeke 2008). We selected a mortality submodel similar to Vanoverbeke (2008) and Rinke and Vijverberg (2005) where death occurs when organisms' mass fall below some threshold of its pervious maximum mass. We selected a critical threshold (V_{crit}) of 40% of maximum weight achieved so far, after which individuals experience a high per capita death rate of (0.35 d^{-1}) (Rinke and Vijverberg 2005).

Parameterization

The scaled DEB model used by DEB-IBM has eight parameters, with two additional parameters needed for the ageing sub-model, and two parameters for the feeding sub-model (Table 1). The processes in DEB theory are abstractions; therefore most of the parameter values cannot be measured directly. Rather, parameters influence various fluxes, which influence observable output like body size over time, reproduction, or survival (Kooijman 2010, Nisbet et al. 2012). However, DEB model parameters for a species can be obtained by fitting the model to observed life-history traits over time. We used a data set for *Daphnia magna* comprising individual growth and reproduction data at four food levels (Sokull-Kluettgen 1998) (details of parameterization given in appendix 1).

Simulation experiments

Simulations were designed to mimic the experimental settings described in Preuss et al. (2009). Population dynamics were driven by "semi-batch" feeding conditions, i.e. food was added each day Monday – Thursday, and 3x the normal food level on Friday to a 900ml beaker. Three times a week the population was counted in three size classes. The experimental data sets consisted of two experiments conducted at a "low" food level (0.5 mgC d^{-1}), starting with either 5 neonates < 24hrs old ("lowN") or 3 adults and 5 neonates (lowNA), and one experiment conducted at "high" food level (1.3 mg C d^{-1}) that began with 3 adults and 5 neonates (highNA), resulting in three treatments, with 4 replicates each. For each experimental setup, we ran 100 simulations and compared the mean, maximum, and minimum of the simulation runs to the data over the course of the 42 days. For details of the experimental setups in the model, see the ODD model description in the Supplementary Material.

Stochasticity enters the simulations in three ways. First, all mortality either due to ageing or starvation is probabilistic. Secondly, individuals vary in parameter values. We followed the method used in Kooijman et al. (1989) where individuals have a log-normally distributed scatter multiplier which affects the maximum surface area specific assimilation rate. This parameter is scaled out of the model, however following the covariation rules of parameters in DEB theory, the parameters (g, $U_H^b, U_H^p, \dot{J}_{XAm}$, and K) are all affected by the scatter multiplier (Kooijman 1989; Martin et al. 2012; and ODD of this manuscript). Lastly, we assume the amount of food added each day varies due to experimental error with a standard deviation equal to 10% of the desired food concentration.

Our initial comparison of model output and data revealed a mismatch between the model and data. This mismatch was not resolved by changing the model parameters within their confidence intervals. Our conclusion for this mismatch was that the dynamics of the starvation mechanism are poorly understood, and that food-dependent mortality is not modeled accurately by the standard threshold starvation model of DEB theory. In the results section we therefore discuss and test several new alternative size-selective submodels of food-dependent mortality. Moreover, we found that those model individuals that shrink due to food shortage, but do not die, recover much more slowly than real *Daphnia*. We therefore also formulated and tested a revised recovery model.

Results

Individual-level parameterization

Parameterization revealed that the parameters g and $\dot{v}$ co-varied, i.e. they could not be specified individually but their ratio was well determined (Appendix 1, figure 1). This indicates that, at least for *Daphnia* in the given settings, one of these parameters is redundant. An increase in $\dot{v}$ and g together indicates an increasing rate of reserve mobilization, and simultaneously a decrease in the size of the reserves. As both parameters increase towards infinity, one ultimately ends up with a "reserveless" DEB model.

To determine the population-level effect of using different values for parameters linked to the reserve dynamics, we ran simulations using parameter sets where the value of g was fixed at incrementally higher values and all other parameter values estimated (Appendix 1). We found that using fixed values of g within the likely range (10 to infinity) had negligible influence on population level output. Therefore the results from our analysis would be independent on the value chosen for g. We thus used the parameter set with g fixed at 10 for all further simulations. Using the resulting parameter set, the DEB model explained most of the variation in growth and reproduction (Figure 1).

Population-level results for the "standard" DEB-IBM Daphnia model

The model closely matched observations during the initial population growth phase, capturing population growth rate, size distribution, and peak population density for all experimental settings (Figure 2 for the lowN setting; results for all others are in the Supplementary Material). However, after the initial population peak, model predictions and data diverged. We quantified the overall fit by dividing each time series into two periods, the population growth phase ("Growth Phase") and the population decline phase ("Decline Phase"). All predictions after the population peak in the simulations were grouped into the Decline Phase, and all before into the Growth Phase. We then compared overall agreement of the predictions and observations of total density and the three size classes for each of the two periods, for all experimental setups (Figure 3). As a way of comparing goodness-of-fit we report "prediction" r-squared values for each period (Growth and Decline Phases), as well as for the data set as a whole (see Appendix 1). Our analysis revealed a much poorer fit between model predictions and observations during the Decline Phase (Table 2).

Further analysis of the simulation revealed that starvation probability was highly skewed towards larger body sizes. *Daphnia* that died from starvation in the simulations were on average greater than 90% of the length of the largest *Daphnia* in the experiment for all three population experiments. Further analysis revealed that dynamics were highly sensitive to the value of the parameter describing the shrinking threshold for starvation (V_{crit}). For lower values of this parameter, almost no starvation occurred, and for larger values (>0.6) the majority or occasionally all *Daphnia* in an experiment would starve (data not shown). Additionally, the dynamics were "choppy" in that the dynamics was characterized by periods of no death via starvation, intermitted by bursts of many *Daphnia* (typically the largest in the simulation) dying in a short period.

Alternative models of starvation and recovery

We implemented an additional starvation submodel, where mortality was inversely linked to reserve density, *e*, which is a time-weighted average of feeding history (see ODD model description in Supplementary Material):

$$\Pr(mortality)d^{-1} = M(1-e)$$

To check whether starvation was size-selective in the experimental systems, we compared three versions of this new submodel by applying it only to juveniles (negative size selection, NegSS), only to adults (positive size selection, PosSS), or to all *Daphnia* (neutral size selection, NeutSS).

Because we also wanted some indication of how well the starvation models, once parameterized, were able to capture the dynamics of population in other experimental settings, we restricted our paramterizaton data set to one of the population experiments (lowN). We then compared the goodness of fit of the three starvation submodels and to the complete data set (all three population experiment setups) (see Appendix 1 for parameterization and statistical details).

Furthermore, standard DEB theory assumes that a *Daphnia* that has shrunk to, for example, 50 percent of its previous maximum mass behaves physiologically the same as a *Daphnia* that has not shrunk with the same state. This is, however, in disagreement with experimental observations at the individual level, as *Daphnia* recover mass much faster than expected following the standard DEB equations (Perrin et al. 1990; Bradley et al. 1991). One possible explanation is that although *Daphnia* shrink they maintain their ability to ingest and assimilate energy according to their previous maximum size. This may be due to the fact that *Daphnia* do not shrink in physical length, as they live within a ridged carapace, and thus their feeding appendages keep their previous size even as the mass of the *Daphnia* shrinks. This can be modelled in DEB by using the maximum achieved value of length in the assimilation formula. By using this modified recovery model, we found (data not shown) a large improvement in predictions for the timing of individual-level recovery from compared to data from Perrin et al. (1990). Although both models underpredict time to recovery compared to the data, the “fast” recovery model predicts a time to recover (4 days) much closer to the data (between 1-3 days) than the “de□a□t” reco□ery (□days□□

Population-level results for the modified DEB-IBM model

Parameterization of the three starvation submodels on the lowN dataset resulted in values of 0.085, 0.39, and 0.090 d^{-1} for *M*, the mortality constant for the NeutSS, PosSS, and NegSS sub-models, respectively. The NeutSS (R^2 0.938) and NegSS (R^2 0.929) submodels led to substantially better fits on the paramterization data set (lowN) than the PosSS (R^2 0.638). On the complete data set (all three population experiments), all three modified starvation submodels better matched the data relative to the standard model and most of this improvement in model fit relates to increased predictive power during the Decline Phase (Table 2). While the NeuSS and NegSS models fit the parameterization data set nearly equally (Supplementary material figure 5A), the NegSS model provided the best fit to the complete data set (Table 2). This was driven by a better agreement of model and data for the independent data sets, specifically for the highNA experiment (Figure 4).

The results of the starvation recovery submodel showed an improved fit over the standard recovery model (Figure 5). This result is mainly due to the lack of production of offspring for the standard dynamics compared to the revised model and experimental observations. This lack of production of new offspring ultimately then leads to no *Daphnia* in the intermediate size class, and results in a population dominated by large *Daphnia*.

Discussion

Having a generic model relating population dynamics to the size, maturity, energy reserves, and current food intake of its constituent organisms would raise Individual-based Ecology (IBE) to a completely new level. IBE would be then based on firm and increasingly tested theory. Species would still be expected to show different physiological and behavioral strategies, but with IBMs based on DEB theory or any other kind of generic theory, we would have a much better idea of where and when to use standard approaches, and where to look for more specific submodels. This might even help to establish similar standard models at the behavioural level (e.g. Imron et al. *in press*).

Did our attempt to predict population dynamics from what individuals do indicate that DEB theory is such a generic theory for IBE? The answer is: yes and no. On the one hand, the standard DEB model without *ad hoc* modifications accurately predicted the population growth rate and peak density of laboratory *Daphnia* populations in different conditions from a model parameterized at the individual level. This suggests that the DEB model with little modification may be used for many applied purposes when an understanding of how population growth rate varies as a function of the environment is required. For example in ecotoxicology, population growth rate often is proposed as a composite indicator of toxicity of chemicals, which takes into consideration simultaneously reductions in growth, reproduction, and survival (Forbes and Calow 2002). DEB theory can easily be used to link individual performance under toxicant stress to effects on the population growth rate (see Jager and Klok 2010), and thus this work further supports its use. Additionally, because the model was able to predict growth rate at multiple food levels, our work provides support for extrapolation of toxic effects on population growth rate to other food levels, an important pattern emerging on population level (Preuss et al. 2010).

On the other hand, the unmodified model did not accurately capture the dynamics after the population peak, where there was little food per *Daphnia*. In contrast to the model predictions, the experimental observations showed a sharp decline in *Daphnia* density. This decrease in density also decreased competition for food allowing those *Daphnia* that survived to consume more, and thus grow at faster rates. Because of this we saw a discrepancy not only in the population density between model predictions and observations, but also in the size distribution. In the experiments, surviving *Daphnia* move relatively quickly from one size class to another, however in the model simulations *Daphnia* generally got stuck at the juvenile stage and do not reach maturity because they do not receive enough food.

This result highlights the problem that although DEB theory has been tested extensively at the individual level, few such tests have been conducted at very low (or decreasing) food densities, or evaluated performance of individuals after recovering from long periods of starvation. This is true not only for DEB, but also for other theories which hope to extrapolate from the individual to higher levels of organization such as more traditionally formulated, empirically-based “bioenergetic” models which are often used in fisheries research (Nisbet et al. 2012). The issue seems to be a lack of experiments or data on response of individuals experiencing food shortage.

The discrepancy between model predictions and observations for declining populations turned out to be highly informative. It was our hope that cross-level testing DEB would lead us to identify potential limitations of standard DEB theory and possibly find ways to overcome these limitations. Due to the lack of data on starvation, we had to do this inversely, i.e. infer from population-level patterns to the individual-level process of starvation. We contrasted three phenomenological starvation models, which differed in their size selectivity. We found that if we assumed negative size selection, i.e. starvation of smaller individuals, agreement between predicted and observed population dynamics and structure were improved. One notable contradiction between predictions and observations for the PosSS model was a lack of neonate production after the initial population growth phase. This trend is best observed in the high food level experiment (Figure 4). While there was a relatively good fit for the average total abundance during the decline phase, we can clearly see this was a case of a good fit for the wrong reason. Unlike in the experiments, there was no production of neonates. This is due to the fact that under conditions where adults are more sensitive to starvation than juveniles, no individuals that can reproduce remain once conditions recover. The NeutSS model captured the dynamics and size structure of the population in that it predicted bursts of neonate production, however, compared to the NegSS model, these burst were too small as there were fewer adults due to the non-size selective mortality. Consequently, prediction of neonate production in the NegSS model was most appropriate, leading also the more accurate predictions of the total population abundance (Table 1; Figure 3b).

Our size-selective starvation model was *ad hoc*, representing our inference from mismatches between model predictions and data. Note that without using the other standard elements of the DEB model, this mismatch could have been ascribed to any element of the model, whereas here we were immediately led to focus on starvation. The outcome of our analysis is supported by the analysis conducted previously on the same population dataset using an empirical individual-based population model (Preuss et al. 2009), in which the decline of the population density after the peak was explained as a mixture of starvation and crowding. Crowding is thereby a mixture of negative interference (Goser and Ratte 1994) and physical contact of the daphnids, leading to life-strategy shifts and reduced feeding even at the same level of food (Goser and Ratte 1994, Cleuvers et al. 1997). Within this empirical model a crowding submodel was used, calibrated on individual level data. One of the main factors in this crowding submodel was the increased mortality of juveniles (Preuss et al. 2009) as was also found in this analysis and attributed to starvation.

Increased juvenile food-dependent mortality was proposed in a different model and experimental system to be important for capturing another aspect of *Daphnia* populations .(McCauley *et al.* 2008). It has been found in experimental systems (McCauley *et al.* 1999; McCauley *et al.* 2008) that when *Daphnia* feed on a dynamic prey source, the *Daphnia* population and is algal resource may exhibit either small (SA) amplitude cycles or large amplitude (LA) cycles. Replicate populations may exhibit either dynamic pattern and on occasions may alternate between these two multiple attractors. When cycles are observed in the field, the predominant pattern is SA cycles (Murdoch *et al.* 1998). Besides the magnitude of the fluctuations the key diagnostic feature of the two cycle types is that in SA cycles, the juvenile development time (time from birth to reproducing adult) is longer than the period of the population cycles, while in the LA cycles the juvenile development time is shorter then the cycle period (McCauley et al. 2008).

To explore the origin of these dynamics, McCauley et al (2008) developed a deterministic, two-stage-structured (juveniles and adults) bioenergetic model that includes food-dependent mortality rates estimated separately for adults and juveniles. Their parameterization generated higher food-dependent mortality coefficients for the juvenile stage class than the adults. However, more recently it was realized that it was specifically the higher juvenile food-dependent mortality was key to observing both cycle types. The stabilizing mechanism responsible for generating the small amplitude cycles was the presence of adults that survived through the population decline phase and were able to reproduce shortly after the algae population began to recover (Ananthasubramaniam et al 2011). This is remarkably similar to the pattern we see in the high food experiment where the bursts of neonate production observed during the Decline Phase and the subsequent leveling off of the population decline were only predicted by the NegSS model.

To test if our model captures, without any further calibration or model modification, the SA/LA cycle patterns explored by McCauley et al. (2008), we used the NegSS model, but instead of simulating the populations in “batch-fed” environments, we let them feed on a prey following logistic growth. In agreement with previous models, the populations exhibit exclusively SA cycles when they carrying capacity of prey is low, and LA cycles when the carrying capacity of the prey is high. Most interestingly, the model also captures the dynamic at intermediate prey carrying capacities where the population exhibits the multiple attractors (LA and SA cycles) proposed for previous models and observed in the lab populations. Particularly convincing is that as in experimental observations, the model also captures they key diagnostic feature, or pattern, that under SA cycles the mean juvenile development time was longer than the cycle period, while the opposite was found for LA cycles (Figure 6). We take this finding as strong evidence that our modified DEB model is a realistic and comprehensive representation of laboratory *Daphnia* populations, which is able to reproduce population level patterns for a wide range of environmental settings.

In addition to the size selective nature of food-dependent starvation risk we also investigated the consequence of assumptions of recovery after a long period of starvation. The standard DEB model does not distinguish between “novel” somatic growth and recovery somatic growth. We tested this assumption against individual level data (Perrin et al. 1990), and revealed that this assumption grossly underestimated recovery of somatic mass. We thus used an alternate assumption where recovering individuals retain the performance abilities of their previous maximum size. This modified model performed much better at both levels of biological organization tested, however recovery of somatic growth was still underestimated at the individual level. With the new assumption adult *Daphnia* were able to assimilate food more quickly when food levels began to recover, resulting in neonate production in agreement with observations from the lowNA and to a greater extent, highNA experiments. The poor performance of the default recovery submodel highlights the fact that “novel” and “recovery” somatic growth cannot be treated as equivalent.

The goal of our study was to test whether simple, non-species specific, models in an IBM context can be used to predict and understand the dynamics of populations. A general model approach, as for example DEB, comes always to a price. Describing species by a general approach means that flexibility to describe the response of the species in detail is reduced. For example in DEB energy fluxes are described by rates in scaled proportions, which means that the parameters cannot be measured directly nor compared to measured data in contrast to other approaches which are explicitly developed to simulate daphnids (Rinke and Vijverberg 2005; Vanoverbeke 2008; Preuss et al. 2009). There are many aspects of *Daphnia* physiology and behavior not included in our model: food dependent filer-area adaptation (Lampert 1994), food and maternal influences of the size of offspring at birth (Glazier 1992), non-food related crowding effects on filtration rates and survival (Matveev 1993; Boersma et al. 1999; Preuss 2009), and discontinuous growth due to molting (Vanoverbeke 2008). Nevertheless, with our simple, non-species specific individual-based implementation of DEB theory we were able to capture many quantitative and qualitative patterns of *Daphnia* population dynamics. Additionally, our analysis suggests that DEB theory can be further simplified for use in a population context, as there were negligible differences between the predictions of the DEB model with and without reserves at the population level (Appendix 1, figure 2). This simplification eliminates one parameter and one state variable from the model (see formulation in supplementary material).

How general the modified submodels resulting from our modeling exercise are among other taxa remains to be seen. But our work clearly highlights the importance of the starvation mechanism for capturing the dynamics of population in time. Additionally, this work demonstrated the need to confront general theories with data across different levels of organization. We hope our work serves to motivate further experimental work and model development with the ultimate goal of producing a general model of individual performance useful for applied and quantitative purposes at the population level or higher.

Data for both the individual and population level exist for many species, mostly observed in the laboratory. Our study demonstrated that using the generic software DEB-IBM, and generic tools for determining the DEB parameters, is straightforward and quickly leads to important new insights regarding the general theory and regarding the species being considered.

Interestingly, the most productive part of our study was our attempts to understand why predictions from standard DEB theory were sometimes wrong. Theories may, perhaps more often then not, work, i.e. reproduce observed patterns, for the wrong reasons. Trying to understand where a theory fails and why is thus a critical step in theory development. Thus, testing DEB theory across levels may not only raise Individual-based Ecology to a new level, but may also help change our bias towards confirming theories, instead of falsifying them.

Acknowledgements

We thank Bharath Ananthasubramaniam, Florian Hartig, Louise Stevenson, Elke Zimmer for helpful discussions. BTM, TJ, TP, and VG acknowledge support from by the European Union under the 7th Framework Programme (project acronym CREAM, contract number PITN-GA-2009-238148.) RMN acknowledges support from US National Science Foundation under grant EF-0742521, and from the US National Science Foundation and the US Environmental Protection Agency under Cooperative Agreement Number EF 0830117.

References

Ananthasubramaniam, B., R. M. Nisbet, W. A. Nelson, E. McCauley, and W. S. C. Gurney, 2011. Stochastic growth reduces population fluctuations in *Daphnia*-algal systems. Ecology, 92:362–372

Berger, U., H. Hildenbrandt, and V. Grimm. 2002. Towards a standard for the individual-based modeling of plant populations: self-thinning and the field-of-neighborhood approach. Natural Resource Modeling 15:39- 54.

Boersma, M., 1997. Offspring size and parental fitness in *Daphnia magna*. Evolutionary Ecology 11: 439–450.

Bradley, M. C., N. Perrin, P. Calow. 1991. Energy allocation in the cladoceran *Daphnia* magna Straus, under starvation and refeeding. Oecologia 86: 414-418

Cleuvers, M., B. Goser, H. T. Ratte. 1997. Life-strategy shift by intraspecific interaction in *Daphnia magna*: change in reproduction from quantity to quality. Oecologia 110:337–345.

DeAngelis, D. L., and W. M. Mooij. 2005. Individual-based modeling of ecological and evolutionary processes. Annual Reviews of Ecology and Evolutionary Systematics 36:147-168.

de Roos, A. M. 2008. Demographic analysis of continuous-time life-history models. Ecology Letters 11: 1-15.

Forbes V. E., and P. Calow. 2002. Population growth rate as a basis for ecological risk assessment of toxic chemicals. Philisophical Transactions of the Royal Society B 357: 1299-1306

Gergs, A., and H. T. Ratte. 2009. Predicting functional response and size selectivity of juvenile *Notonecta maculata* foraging on *Daphnia* magna. Ecological Modelling 220: 3331-3341.

Glazier, D.S. 1992. Effects of food, genotype, and maternal size and age on offspring investment in *Daphnia magna*. Ecology 73: 910–926.

Grimm, V., 1999. Ten years of individual-based modelling inecology: What have we learned, and what could we learn in the future? Ecological Modelling 115: 129–148.

Grimm, V., T. Wyszomirski, D. Aikman, J. Uchmanki. 1999. Individual-based modelling and ecological theory: synthesis of a workshop. Ecological Modelling 115:275-282.

Grimm, V., Railsback, S.F., 2005. Individual-based modeling and ecology. Princeton University Press, Princeton.

Grimm, V., U. Berger, F. Bastiansen, S. Eliassen, V. Ginot, J. Giske, J. Goss-Custard, T . Grand, S. Heinz, G. Huse, A. Huth, J. U. Jepsen, C. Jørgensen, W. M. Mooij, B. Müller, G. Pe'er, C. Piou, S. F. Railsback, A. M. Robbins, M. M. Robbins, E. Rossmanith, N. Rüger, E. Strand, S. Souissi, R. A. Stillman, R. Vabø, U. Visser, D. L. DeAngelis. A standard protocol for describing individual-based and agent-based models. 2006. Ecological Modelling 198:115-126.

Grimm, V., U. Berger, D. L. DeAngelis, J. G. Polhill, J. Giske, S. F. Railsback. 2010. Ecological Modelling 221: 2760-2768

Hanegraaf, P. P. F., and E. B. Muller. 2001. The dynamics of the macromolecular composition of biomass. Journal of Theoretical Biology 212: 237-251.

Hendriks, A. J. 1995. Modeling Response of species to microcontaminants - comparative ecotoxicology by (sub)lethal body burdens as a function of species size and partition ratio of chemicals. Ecotoxicology and Environmental Safety 32:103-130.

Hou, C., W. Zuo, M. E. Moses, W. H. Woodruff, J. H. Brown, and G. B. West. 2008. Energy uptake and allocation during ontogeny. Science 322: 736-739

Imron, M. A., A. Gergs, and U. Berger. *in press*. Structure and sensitivity analysis of individual-based predator-prey models. Reliability Engineering and System Saftey.

Jager, T., C. Klok. 2010. Extrapolating toxic effects on individuals to the population level; the role of dynamic energy budgets. Philosophical Transactions of the Royal Society B 365: 3531-3540

Kendall, B. E., S. P. Ellner, E. McCauley, S. N. Wood, C. J. Briggs, W. W. Murdoch, and P. Turchin. 2005. Population cycles in the pine looper moth: Dynamical tests of mechanistic hypotheses. Ecological Monographs 75: 259-276.

Kooi, B. W., and S.A.L.M. Kooijman. 1994. The transient-behavior of food-chains in Chemostats. Journal of Theoretical Biology 170: 87-94.

Kooijman, S. A. L. M., N. v. d. Hoeven and D. C. v. d. Werf. 1989. Population consequences of a physiological model for individuals. Functional Ecology 3: 325-336,

Kooijman, S.A.L.M. 2010. Dynamic Energy Budget theory for metabolic organisation. Cambridge University Press, Cambridge.

Lampert, W. 1994. Phenotypic plasticity of the filter screens in *Daphnia*-adaptation to a low-food environment. Limnology and Oceanography 39: 997□1006.

Martin, B. T., E. I. Zimmer, V. Grimm, T. Jager. 2012 (in press). Dynamic Energy Budget theory meets individual-based modelling: a generic and accessible implementation. Methods in Ecology and Evloution.

Matveev, V., 1993. An investigation of allelopathic effects of *Daphnia*. Freshwater Biol. 29: 99□105.

McCauley, E., W. A. Nelson, and R. M. Nisbet. 2008. Small-amplitude cycles emerge from stage-structured interactions in *Daphnia*-algal systems. Nature 455: 1240-1243.

McCauley, E., R. M. Nisbet, W. W. Murdoch, A. M. de Roos, and W. S. C. Gurney. 1999. Large-amplitude cycles of *Daphnia* and its algal prey in enriched environments. Nature, 402: 653-656.

Muller, E. B. 2011. Synthesizing units as modeling tool for photosynthesizing organisms with photoinhibition and nutrient limitation. Ecological Modelling 222: 637-644.

Muller, E. B., R. M. Nisbet, and H. A. Berkley 2010. Sublethal toxicant effects with dynamic energy budget theory: model formulation. Ecotoxicology 19: 48-60.

Murdoch, W. W., R. M. Nisbet, E. McCauley, A. M. de Roos and W. S. C. Gurney. 1998. Plankton abundance and dynamics across nutrient levels: Tests of hypotheses. Ecology, 79, 1339-1356.

Nisbet, R. M., M. Jusup, and T. Klanjscek. 2012 (in press). . Integrating Dynamic Energy Budget (DEB) theory with traditional bioenergetic models. Journal of Experimental Biology.

Nisbet, R. M., E. McCauley, and L. R. Johnson. 2010. Dynamic energy budget theory and population ecology: lessons from *Daphnia*. Philosophical Transactions of the Royal Society B 365: 3541-3552.

Nisbet, R. M., E. B. Muller, K. Lika, and S. A. L. M. Kooijman. 2000. From molecules to ecosystems through dynamic energy budget models. Journal of Animal Ecology 69: 913-926.

Pecquerie, L., L. R. Johnson, S. A. L. M. Kooijman, and R. M. Nisbet. 2011. Analyzing variations in life-history traits of Pacific salmon in the context of Dynamic Energy Budget (DEB) theory. Journal of Sea Research 66: 424-433.

Pecquerie, L., P. Petitgas, and S. A. L. M. Kooijman. 2009. Modeling fish growth and reproduction in the context of the Dynamic Energy Budget theory to predict environmental impact on anchovy spawning duration. Journal of Sea Research 62:93-105.

Perrin, N., M. C. Bradely, P. Calow. 1990. Plasticity of storage allocation in *Daphnia magna*. Oikos 59: 70-74.

Preuss, T. G., M. Hammers-Wirtz, U. Hommen, M. N. Rubach, and H. T. Ratte. 2009. Development and validation of an individual based *Daphnia magna* population model: The influence of crowding on population dynamics. Ecological Modelling 220: 310-329.

Preuss, T. G., M. Hammers-Wirtz, and H. T. Ratte. 2010. The potential of individual based population models to extrapolate effects measured at standardized test conditions to relevant environmental conditions-an example for 3,4-dichloroaniline on *Daphnia magna*. Journal of Environmental Monitoring 12: 2070-2079.

Preuss, T. G., M. Telscher, and H. T. Ratte. 2008. Life stage-dependent bioconcentration of a nonylphenol isomer in *Daphnia* magna. Environmental Pollution 156: 1211-1217.

Railsback, S. F., and V. Grimm. 2012. Agent-based and individual-based modeling: a practical introduction. Princeton University Press, Princeton, New Jersey.

Rinke, K., and J. Vijverberg. 2005. A model approach to evaluate the effect of temperature and food concentration on individual life-history and population dynamics of *Daphnia*. Ecological Modelling 186: 326-344.

Ross, A. H., and R. M. Nisbet. 1990. Dynamic-models of growth and reproduction of the mussel *Mytilus-edulis-l*. Functional Ecology 4: 777-787.

Saraiva, S., J. van der Meer, S. A. L. M. Kooijman, and T. Sousa 2011. DEB parameters estimation for *Mytilus edulis*. Journal of Sea Research 66: 289-296.

Sokull-Kluettgen, B., 1998. Die kombinierte Wirkung von Nahrungsangebot und 3,4-Dichloranilin auf die Lebensdaten von zwei nahverwandten Cladocerenarten, *Daphnia magna* und *CerioDaphnia quadrangula*. Shaker, Aachen.

Sousa, T., T. Domingos, J. C. Poggiale, and S. A. L. M. Kooijman. 2010. Dynamic energy budget theory restores coherence in biology. Philosophical Transactions of the Royal Society B 365: 3413-3428.

van Haren, R. J. F., and S. A. L. M. Kooijman. 1993. Application of the dynamic energy budget model to *Mytilus edulis (L.)*. Netherlands Journal of Sea Research, 31, 119-133.

van Leeuwen I. M. M., J. Vera, O. Wolkenhauer. 2010. Dynamic energy budget approaches for modelling organismal ageing. Philosophical Transactions of the Royal Society B 365: 3443-3454

Vanoverbeke, J. 2008. Modeling individual and population dynamics in a consumer-resource system: Behavior under food limitation and crowding and the effect on population cycling in *Daphnia*. Ecological Modelling 216, 385-401.

Wilensky, U. 1999. NetLogo. http://ccl.northwestern.edu/netlogo/. Center for Connected Learning and Computer-Based Modeling, Northwestern University, Evanston, IL.

Woodward, G., D. M. Perkins, and L. E. Brown. 2010. Climate change and freshwater ecosystems: impacts across multiple levels of organization. Philosophical Transactions of the Royal Society B 365: 2093-2106.

Tables

Table 1. Parameters of the DEB model for *Daphnia magna* along with the confidence intervals determined via profile likelihoods. The unit for time (t) is days, for structural length of animals (L) in mm, for the abundance of prey (#) in cells, and for length of the environment (l) in cm.

symbol	Description	dimension	value	95% confidence interval
	DEB parameters			
□	Fraction of mobilized energy to soma	-	0.678	.657-.700
□$_R$	Fraction of reproduction energy fixed in eggs	-	0.95	Fixed value
$\dot{k}_m$	Somatic maintenance rate coefficient	t^{-1}	0.3314	0.327 - 0.336
$\dot{k}_j$	Maturity maintenance rate coefficient	t^{-1}	0.1921	0.150-0.236
U_H^b	Scaled maturity at birth	tL^2	0.1108	0.0989 - 0.123
U_H^p	Scaled maturity at puberty	tL^2	2.555	2.36 - 2.844
$\dot{v}$	Energy conductance	Lt^{-1}	18.1	17.89 - 18.3
g	Energy investment ratio	-	10	Fixed value
	Ageing parameters			
$\ddot{h}_a$	Weibull ageing acceleration	t^{-2}	3.04E-6	1.70E-6 - 4.60E-6
s_G	Gompertz stress coefficient	-	.019	.00911-.0273
	Prey dynamics parameters			
$\{\dot{J}_{XAm}\}$	Surface-area-specific max ingestion rate	$\#L^{-2}t^{-1}$	3.80E+05	3.7E+5 - 4.0E+5
K	Half-saturation coefficient	$\#l^{-3}$	1585	1571 - 1600
	***Daphnia* specific parameter values**			
Molt-time	Time between reproductive events	t	2.8	-
V_{crit}	Proportion of structural mass below which *Daphnia* experience starvation mortality	-	0.4	-
M	Reserve dependent mortality coefficient	t^{-1}	varied	-

Table 2. R^2 values for the default DEB-IBM and various adapted models the before (Growth Phase), after (Decline phase) the population peak, and the entire data set for total abundance, and each of the 3 size classes, over 42 day population experiments at 3 experimental setting. Additionally the negative log-likelihood ($-\ell$) is given for the Standard DEB model and the three modified mortality submodels.

	R^2			$-\ell$
	Growth Phase	Decline Phase	Total	Total
Standard DEB model	0.878	-0.2013	0.318	199643
Food-dependent mortality sub-models				
Neutral (all)	0.920	0.873	0.903	28249
Negative (juveniles only)	0.921	0.897	0.916	24358
Positive (adults only)	0.910	0.342	0.618	111757

Figures captions

Figure 1. Data for growth (a) and reproduction (b) at four food levels (100000, 25000, 5000, and 1000 cells/ml) and the DEB model fit. The experiment was conducted in a flow-through system in 500 ml ADAM medium at a flow-through rate of 360 ml h^{-1}.

Figure 2. Comparison of data and DEB-IBM predictions at the population level for the lowN experiment. Experiments were initiated with 5 neonates in a 900ml beaker, and 0.5mgC was added per day. Simulations with DEB-IBM replicated the experimental conditions. Figures show the mean (think black line) and max and min (dashed grey lines) of 50 simulations. Simulations for the lowNA and highNA experiments are shown in figure 1 of appendix 3.

Figure 3. Observed vs predicted values for all 3 population experiments for total abundance (black circles), and three size classes: large (red diamonds), juveniles (blue squares), and neonates (green triangles) for the standard model (a) and the adapted model (NegSS) with the additional juvenile food-dependent mortality submodel (b). The data are divided into two panels, for data before the population peak (Growth Phase), and after (Decline Phase).

Figure 4. Comparison of the performance of three starvation submodels with data from the highNA experiment. In each of the three models, a 1 parameter food-dependent mortality submodel, was applied, but models differed in that it was either applied only to juveniles (black solid), only adults (black dashed), or all *Daphnia* (grey solid). Simulations for the lowN and lowNA experiments are shown in figure 2 of appendix 3.

Figure 5. Comparison of alternate starvation-recovery assumptions against the highNA data set. The grey line show the scenario where individuals feed at a rate proportional to their current length, while the black line shows the average of 100 model simulations when individuals feed at a rate proportional to their maximum length attained. Simulations for the lowN and lowNA experiments are shown in figure 3 of appendix 3.

Figure 6. Two characteristic simulations, showing the switches between multiple attractors of LA and SA cycles. Simulations were runs using the NegSS model where the *Daphnia* feed on a prey source following logistic growth (r = 1.5, K = 5e-5 mgC ml^{-1}) in a 30 liter system. Simulations were initiated with 5 neonate *Daphnia*.

Figures

Figure 1.

A.

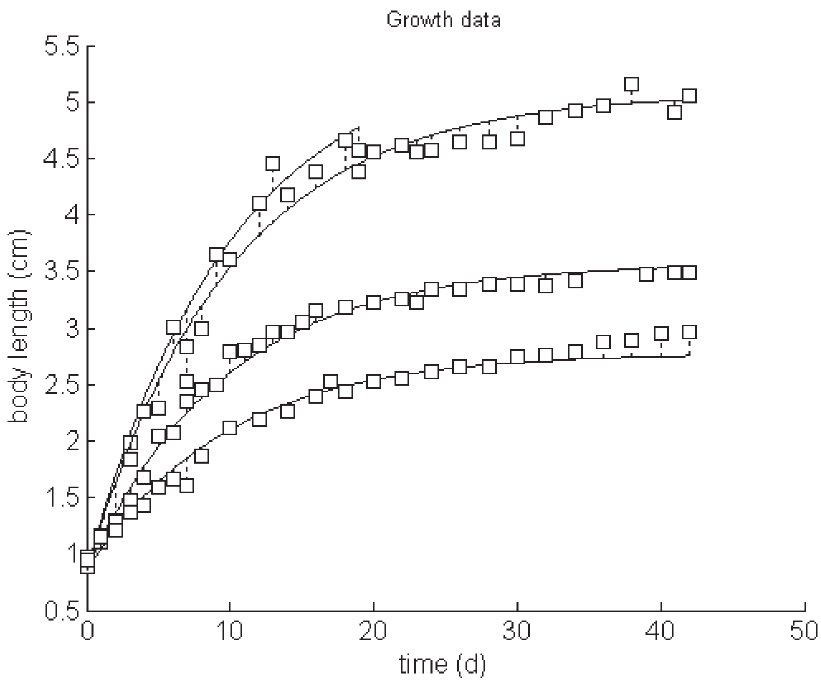

B.

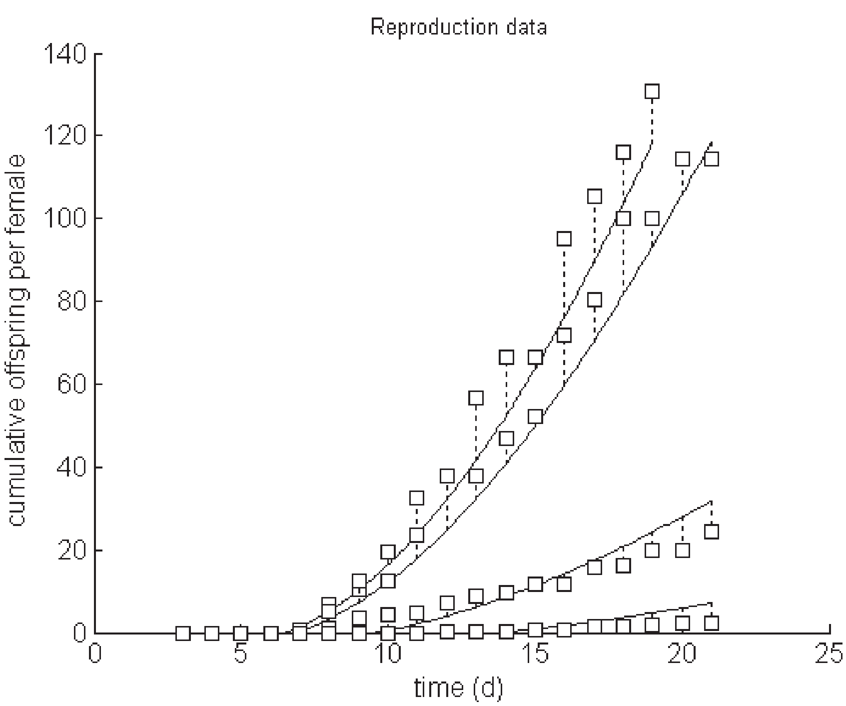

Figure 2

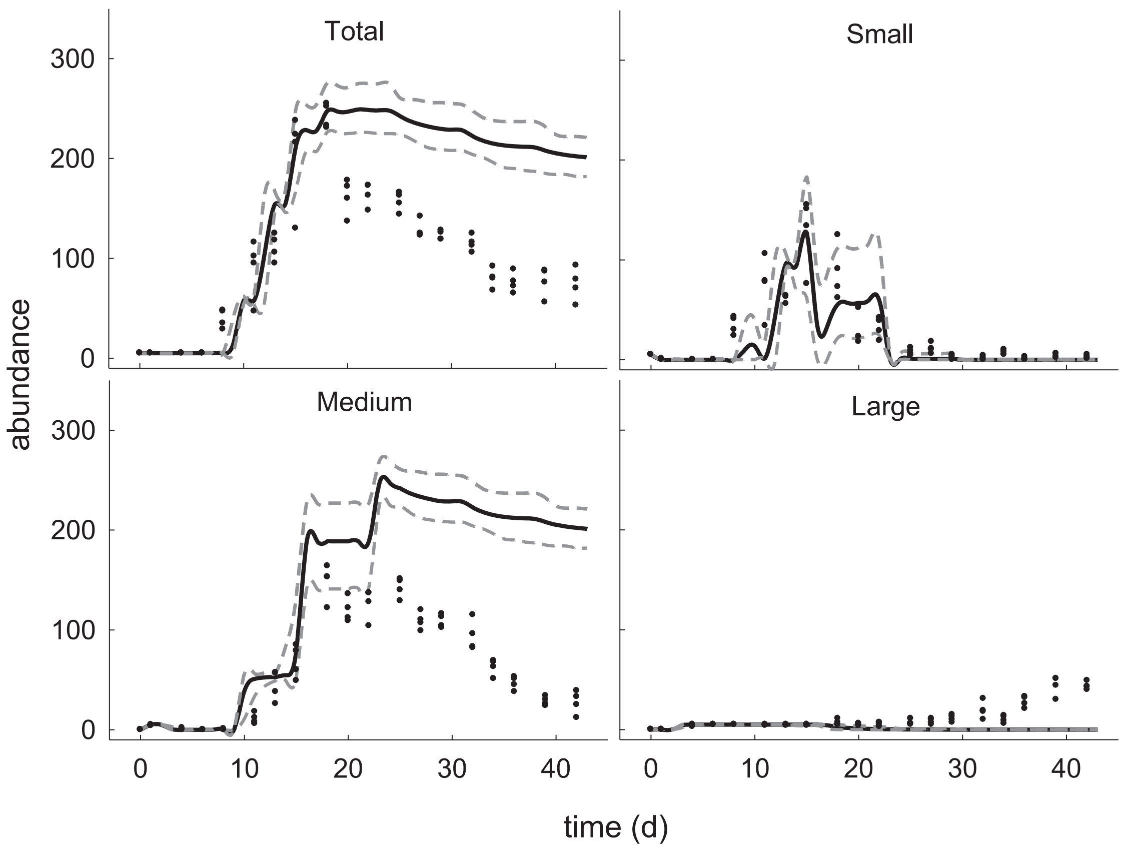
Total
Small
Medium
Large
abundance
time (d)
0
100
200
300
0
10
20
30
40

Figure 3.

A.

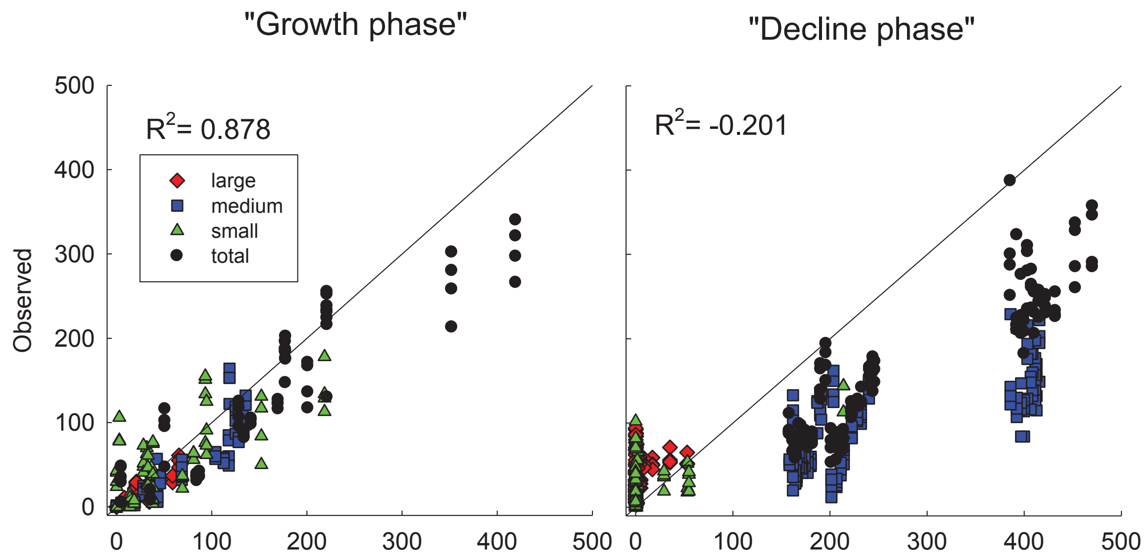
"Growth phase"
"Decline phase"
R²= 0.878
R²= -0.201
large
medium
small
total
Observed
0
100
200
300
400
500

B.

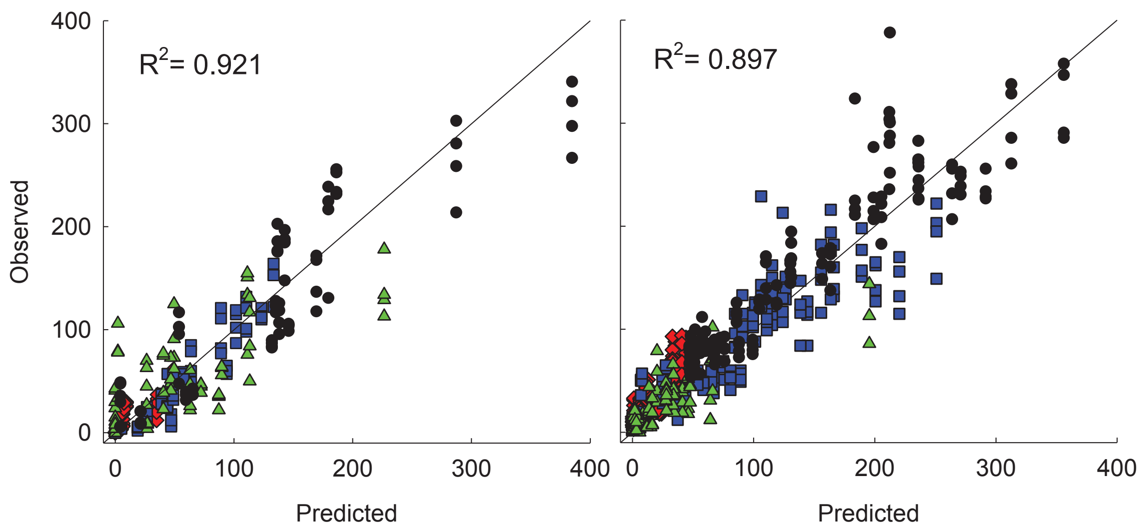
R²= 0.921
R²= 0.897
Observed
Predicted
Predicted
0
100
200
300
400

Figure 4.

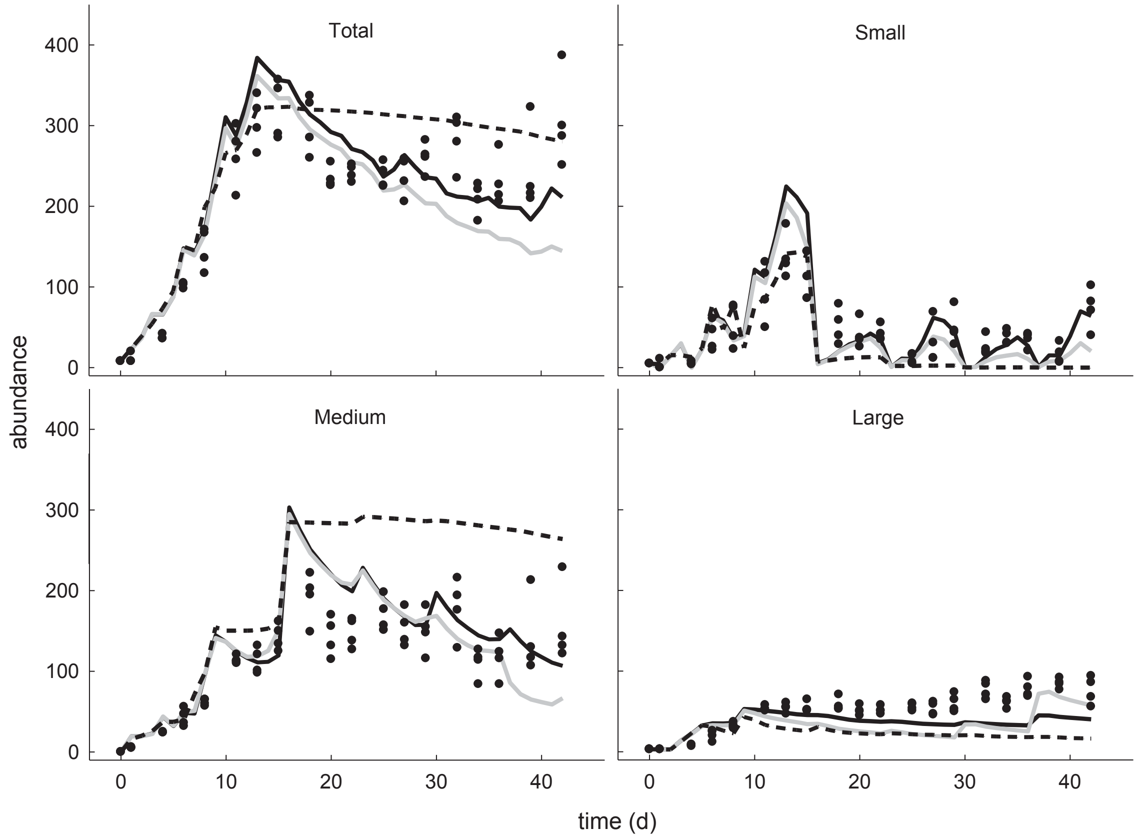
Total
Small
Medium
Large
abundance
time (d)
0
100
200
300
400
0
10
20
30
40

Figure 5.

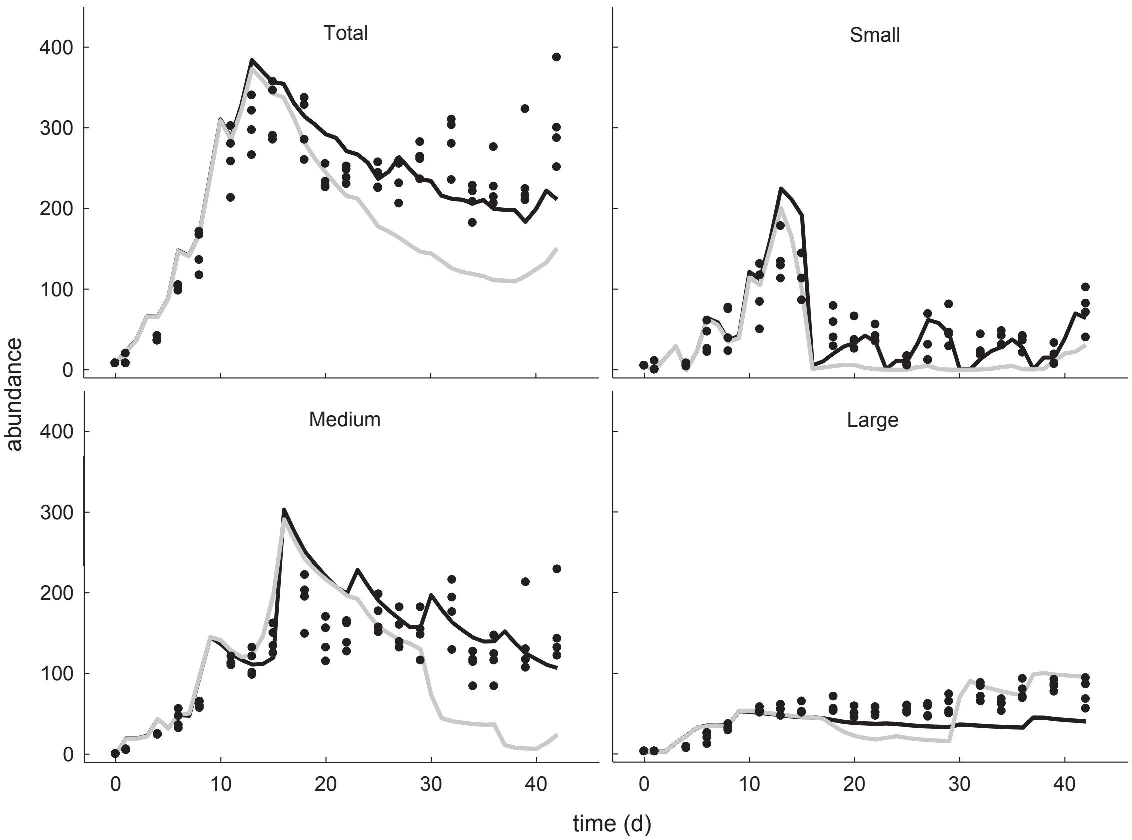
Total
Small
Medium
Large
abundance
time (d)
0
100
200
300
400
0
10
20
30
40

741 Figure 6.

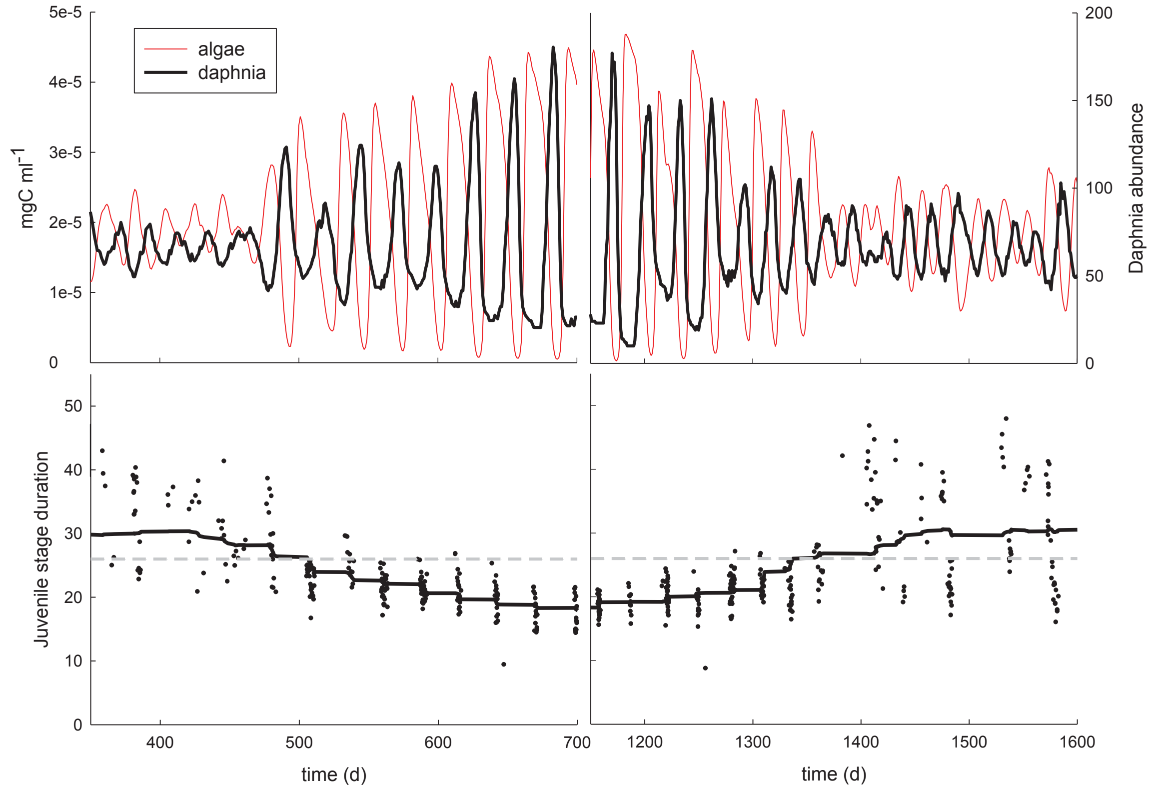

742

Appendix 1. Model parameterization

Parameterization of the DEB model was conducted using the DEB3 version of DEBtox (http://www.debtox.info/debtoxm.php) developed by Tjalling Jager. The data used for parameterization for all parameters except $\{\dot{J}_{XAm}\}$ and the two ageing submodel parameters consisted of body size and reproduction data at 4 food levels over the course of 42 days (Sokull-Kluettgen 1998).

The DEB-IBM has 8 basic parameters, plus 2 parameters for the foraging submodel, and 2 parameters for the ageing submodel. The strategy we employed was to first specify the basic DEB parameters, and then specify the parameters of the two submodels. Of the 8 basic DEB parameters, we fixed one of the parameters: the conversion efficiency from the reproduction buffer to embryonic reserves, κ_R, at 0.95. The parameter was fixed at a high value because the reproduction buffer and the reserves of an embryo are assumed in DEB theory to have the same composition and thus there is a high conversion efficiency. Our parameterization began my simultaneously estimating the remaining 7 DEB parameters (κ, $\dot{k}_M$, $\dot{k}_j$, U_H^b, U_H^p, $\dot{v}$, and g). Additionally we allowed the scaled food density parameter, *f*, to be estimated separately for each food level. The variable, *f*, takes a value between 0 (no feeding) and 1 (feeding at the maximum rate). The value is dependent on the ambient food level and is generally determined by some functional response. When the food levels are known, one can estimate the half-saturation coefficient (*K*) of the scaled Holling type 2 functional response:

$$f = \frac{X}{K + X}$$

While the food levels were known, we instead let *f* be estimated independently for each food level. This is because it is known that over longer time periods daphnia can modify their feeding appendages to forage at higher rates at low food conditions, thus imposing a Holling type 2 functional response would lead to an imperfect fit and we did not want the basic DEB this lack of fit to be compensated for in the 8 DEB parameters. Thus after we determined the 8 DEB parameters of an individual, we fixed these values and then parameterized *K*, with all other parameters fixed. Ageing parameters ($\ddot{h}_a$, s_G) were determined from survival data of 10 individually cultured daphnia at three food levels (0.2, 0.05, and 0.01 mg C d^{-1}) (Preuss et al. 2009). Because ageing is dependent on mobilization (utilization of reserves), which is linked to feeding, organisms can age at different rates at different food levels.

Likelihood estimation of DEB parameters

The log-likelihood of one data type, assuming normal independent errors, is given by (see Jager & Zimmer, 2012):

$$\ell\left(\theta \middle| Y, \sigma^2\right) = -\frac{N}{2}\ln\left(2\pi\sigma^2\right) - \frac{1}{2\sigma^2}\sum_{j=1}^{m}\sum_{i=1}^{k_j}\sum_{r=1}^{n_{ij}}\left(Y_{ijr} - \hat{Y}_{ij}(\theta)\right)^2$$

Where an observation Y_{ijr} represents the observation at *i*th time point, for at the *j*th food level, for the *r*th individual. However, in our case we do not have data for each individual, but rather have the means for the body size and reproduction output for individuals at the *i*th time point of the *j*th food level. Thus we cannot estimate σ^2 directly from the data. To circumvent this problem, we use a separate data set where individual measures of growth and reproduction were measured. We then estimate the variance of each data type (growth and reproduction), and fix σ^2 in our estimation procedure. When the variance is known, the first term not longer depends on the model parameters, and thus equation 1 reduces to:

$$\ell\left(\theta \middle| Y, \sigma^2\right) = -\frac{1}{2\sigma^2}\sum_{j=1}^{m}\sum_{i=1}^{k_j}\sum_{r=1}^{n_{ij}}\left(Y_{ijr} - \hat{Y}_{ij}(\theta)\right)^2$$

Then we can work with the means, $\overline{Y}_{ij}$, instead of individual data points, Y_{ijr} :

$$\ell\left(\theta \middle| Y, \sigma^2\right) = -\frac{1}{2\sigma^2} wSSQ_n(\theta; Y)$$

$$wSSQ_n(\theta; Y) = \sum_{j=1}^{m} \sum_{i=1}^{k_j} n_{ij}\left(\overline{Y}_{ij} - \hat{Y}_{ij}(\theta)\right)^2$$

From here getting the log-likelihood of the complete data set, Y_+, is a matter if summing the log-likelihoods of each data set, Y_S:

$$\ell\left(\theta \middle| Y_+\right) = \sum_{S} \ell\left(\theta \middle| Y_S\right)$$

For the growth data set we compared the predictions of the model to the mean size of daphnia for each combination of food level and time. For the reproduction data set we compare the average number of offspring produced between observation intervals to the predictions of parameter set θ integrated reproduction rate over that same interval (see Jager & Zimmer, 2012):

$$wSSQ_n(\theta; Y) = \sum_{j=1}^{m} \sum_{i=1}^{k_j} \left(\frac{n_{ij} - n_{i-1j}}{2}\right)\left(\int_{t_{i-1}}^{t_i} R_j(\tau, \theta) d\tau - \frac{2Y_{ij}}{n_{ij} + n_{i-1j}}\right)^2$$

However for reproduction, only the data before 21 days was used, as after 21 days (after the 5th brood) there was a significant reduction the reproduction rate of daphnia, not accounted for in the DEB model. We did not use this data as we did not want the model fit to be influenced by reproduction data points after the 5th brood, as daphnia in natural contexts rarely survive to produce more than 5 broods.

Survival data used for parameterizing the ageing submodel follows a multinomial distribution. The log-likelihood is given by (see Jager et al., 2011):

$$\ell(\theta; Y) = \sum_{j=1}^{m} \sum_{i=1}^{k_j} \left(Y_{ij} - Y_{i-1j}\right) \ln\left(S_{ij}(\theta) - S_{i+1j}(\theta)\right)$$

Where S_{ij} ist he number of individual at time point *i* of food level *j* and S_{i+1j} is he number of survivors at the next observation time.

Optimization and confidence intervals

Optimization was conducted using a Nelder-Mead simplex method (Nelder and Mead 1965). Confidence intervals were calculated using the profile likelihood method (Venzon and Moolgavkar 1988; Meeker and Escobar 1995) which is more appropriate for non-linear models (Pawitan 2000).

Parameterization of $\{\dot{J}_{XAm}\}$

Once these parameters were fixed we estimated the final feeding submodel parameter, the maximum surface-area-specific feeding rate, $\{\dot{J}_{XAm}\}$. This parameter determines at what rate food (algal cells) are depleted from the environment by daphnia predation. To fit this parameter we used a data set of growth and reproduction at 3 food levels in batch cultures (Coors et al. 2004). In batch cultures, in contrast with the flow through experiments, at all but very high food levels, all or much of the food is removed each day via predation. How much food is depleted is highly dependent on the $\{\dot{J}_{XAm}\}$ parameter, therefore we used this data to estimate this parameter by running simulations replicating the experimental conditions of the Coors experiments, with incrementally increasing values of $\{\dot{J}_{XAm}\}$. Experiments and model were run in 80ml M4-Elendt medium, daphnids were fed daily *D. subspicatus* at one of three different food levels (0.05, 0.075, and 0.2mgC d^{-1}). *Desmodesmus subspicatus* has an average carbon content of 1.95×10^{-8} mgC $cell^{-1}$. After an initial range finding test we evaluated values of $\{\dot{J}_{XAm}\}$ ranging from 2.0 - 5.0×10^{5} (cells $mm^{-2}d^{-1}$) with a resolution of 1×10^{4} .

Maximum likelihood estimation was used to select the appropriate value in the same manner as in the previous section.

Results of individual parameterization

Analysis of the confidence intervals for each parameter revealed that most parameters were well specified within a narrow range with the exception of $\dot{v}$ and *g*. For each of these parameters there was no narrow peak in the profile likelihood, instead that as the values of $\dot{v}$ and *g* were fixed at higher values, the likelihood increases, but at a decreasing rate (figure 1). An increase in these parameters together, indicate an increase in speed in the reserve dynamics as $\dot{v}$ is the mobilization rate of reserves and *g* is a compound parameter

$$g = \frac{[E_G]}{\kappa[E_M]}$$

where $[E_G]$ is the cost to produce one unit of structure, and $[E_M]$ is the maximum reserve density. Thus an increase in $\dot{v}$ and *g* together indicates a faster of rate reserve mobilization, and simultaneously a decrease in the size of the reserves. As both $\dot{v}$ and *g* increase towards infinity, you ultimately end up with a “reserveless” DEB model. Here we no longer have the parameter *g* and *v*, but we use maximum length L_M as a primary parameter. The differential equation for length is then reduced to:

$$\frac{dL}{dt} = \frac{\dot{k}_m}{3}\left(L_M f - L\right)$$

and the equations for maturity and reproduction now only differ in that instead of mobilized energy being allocated to each state variable it is assimilated energy: fL^2.

$$\frac{dU_H}{dt} = \left(1-\kappa\right)fL^2 - \dot{k}_j U_H \quad \text{when} \quad U_H < U_H^p$$

$$\frac{dU_R}{dt} = \left(1-\kappa\right)fL^2 - \dot{k}_j U_H \quad \text{when} \quad U_H \geq U_H^p$$

Based on the confidence profiles of *g* and $\dot{v}$, the goodness of fit was not significantly worse to a range down to 10 for *g*. Because we were unable to specify the value of *g* and *v* exactly we instead fixed the parameter g at 10. For computational reasons, having g fixed to a lower value means we need less resolution in the time steps, thus we wanted to select the lowest possible value. To determine the consequence of fixing g to 10 as opposed to higher values, we also parameterized the model with g fixed to 100 and a reduced model with no reserves (Table 1). We then ran the population simulations using the each of the parameter sets representing increasing speed of reserve dynamics (Figure 2). The resulting comparison indicated that using parameter sets with faster reserve dynamics, or no reserve state variable at all, had negligible effects on the population dynamics.

As the goal was to test DEB theory, we did not want to deviate from the inclusion of reserves. With g fixed to a value of 10 all parameter values were well specified for the standard DEB model (figure 3), the ageing submodel (figure 4), and the feeding submodel (figure 5). Additionally for the feeding submodel we show simulations of growth and reproduction at the individual level at the three batch-fed, food levels (Coors et al. 2004) with the same assumptions of stochasticity as used in the population simulations.

Parameterization and analysis at the population level

We parameterized the new starvation model by fitting the M parameter using the same "multi data type" likelihood approach used for parameterizing the DEB model. However for parameterizing M at the population level, the data sets used were the total abundance and the abundance of three size classes over time. We used weighted Sum of Squares (wSSQ) to normalize variances within and among data types. Residuals between model and data were first weighted by the square root plus one (one was added to avoid division by zero for some observations), as there was higher variance for higher population abundances. After this transformation there was still heteroscedascticity among the data types (total population abundance, and the abundances of the three size classes for the three population experiment), thus we weighted each data type by its variance. In addition to giving the weighted SSQ for each model type, we also present R^2, which was taken as the 1 – root mean square error, with the root mean square error equal to the wSSQ divided by the weighted variance of the data (Kendall et al. 2005). We parameterized each of the three starvation submodels only using data from the lowN treatment. To compare which model best explained the data, we then compared the three mortality submodels using the complete data set.

References

Coors, A., Hammers-Wirtz, M., Ratte, H.T., 2004. Adaptation to environmental stress in *Daphnia magna* simultaneously exposed to a xenobiotic. Chemosphere 56 (4), 395–404.

T. Jager, C. Albert, T. Preuss and R. Ashauer. 2011. General unified threshold model of survival - a toxicokinetic-toxicodynamic framework for ecotoxicology. Environmental Science and Technology 45:2529-2540

Jager, T., and E. I. Zimmer. 2012. Simplified dynamic energy budget model for analysing ecotoxicity data. Ecological Modelling 225:74-81.

Meeker, W. Q., and L. A. Escobar. 1995. Teaching about approximate confidence regions based on maximum likelihood estimations. The American Statistician 49: 48-53

Nelder, J. A., and R. Mead. 1965. A simplex method for function minimization. The computer Journal 7: 308-313

Pawitan, Y. 2000. A reminder of the fallibility of the Wald Statistic: Likelihood explanation. The American Statistican. 54: 54-56

Preuss, T. G., M. Hammers-Wirtz, U. Hommen, M. N. Rubach, and H. T. Ratte. 2009. Development and validation of an individual based *Daphnia magna* population model: The influence of crowding on population dynamics. Ecological Modelling 220: 310-329.

Sokull-Kluettgen, B., 1998. Die kombinierte Wirkung von Nahrungsangebot und 3,4-Dichloranilin auf die Lebensdaten von zwei nahverwandten Cladocerenarten, *Daphnia magna* und *Ceriodaphnia quadrangula*. Shaker, Aachen.

Venzon, D. J., and S. H. Moolgavkar. 1988. A method for calculating profile-likelihood-based confidence intervals. Applied Statistics 37: 87-94

Table 1. Parameter values used in comparing the sensitivity of population dynamics to the speed of reserve dynamics. Increasing values of g mean faster reserve dynamics (i.e. faster turnover of the reserve compartment). For each set we wither fixed g to 10, 100, or removed the reserve compartment completely g = ∞. The unit for time (*t*) is days, for structural length of animals (*L*) in mm, for the abundance of prey (#) in cells, and for length of the environment (*l*) in cm.

symbol	dimension	g fixed at 10	g fixed at 100	reserveless DEB
DEB parameters				
κ	-	0.678	0.682	0.645
κ_R	-	0.95	0.95	0.95
$\dot{k}_m$	t^{-1}	0.3314	0.308	0.3054
$\dot{k}_j$	t^{-1}	0.1921	0.207	0.2109
U_H^b	tL^2	0.111	0.118	0.134
U_H^p	tL^2	2.547	2.80	2.876
$\dot{v}$	Lt^{-1}	18.1	177.4	-
g	-	10	100	-
L_M	L	-	-	5.42
Feeding submodel parameters				
$\{\dot{J}_{XAm}\}$	$\#L^{-2}t^{-1}$	3.80E+05	3.40E+05	3.80E+05
K	$\#l^{-3}$	1585	1511	1505

Figure 1. Confidence intervals for the energy investment ratio, g (A) and energy conductance, $\dot{v}$ (B) using the profile likelihoods method (Meeker and Escobar 1995). For both g and $\dot{v}$ the model fit continued to improve at a decreasing rate as their values increased.

A.

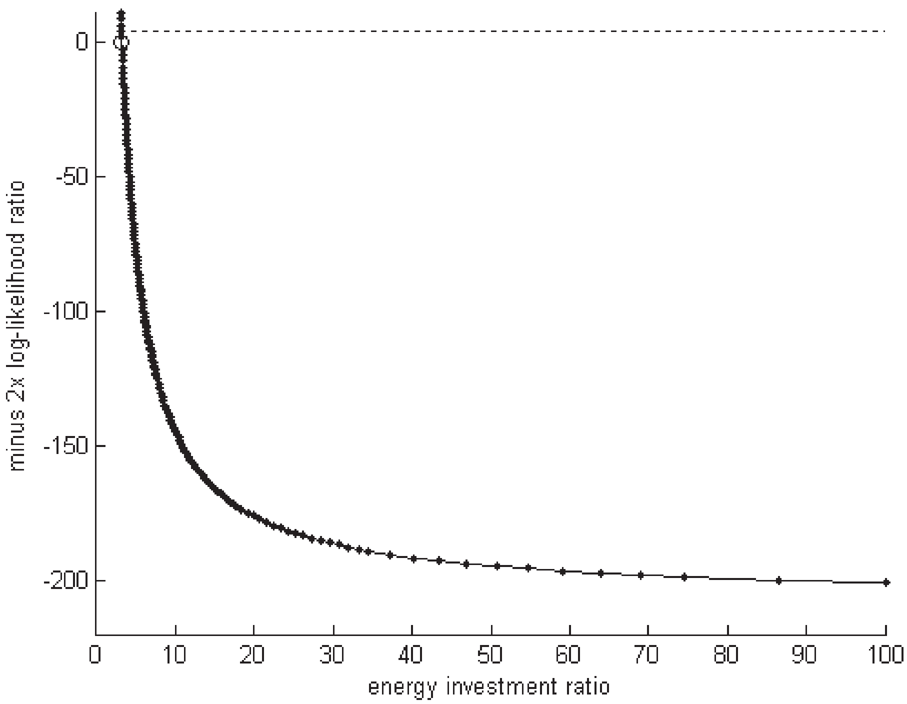

B.

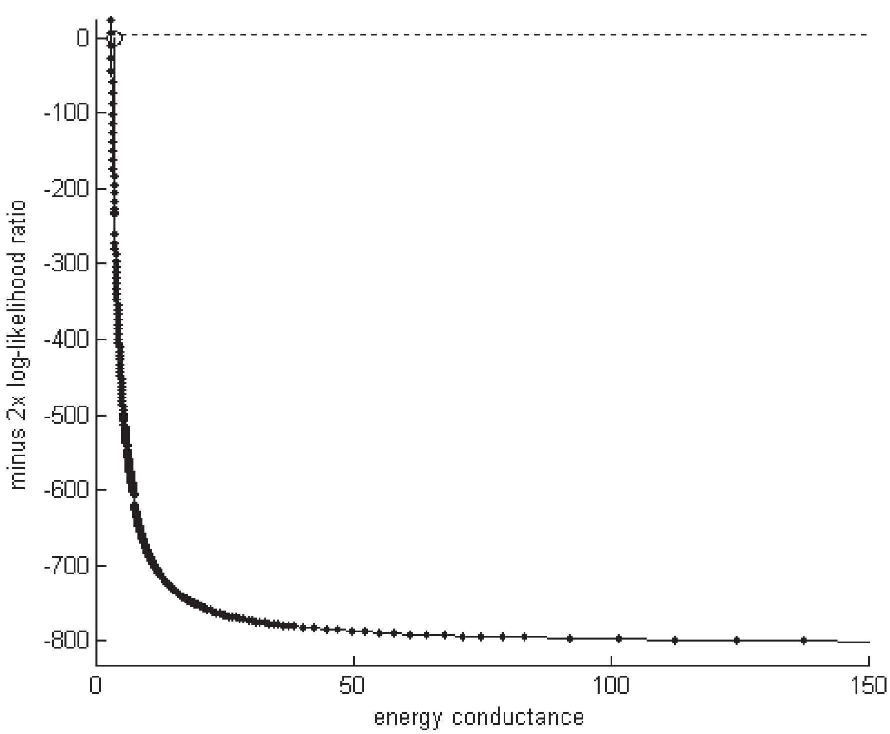

Figure 2. Comparison of mean of 100 simulations of 3 DEB-IBM models parameterized with *g* fixed at 10 (black solid), 100 (grey solid), or the modified reserveless model (black dashed) at the lowN (a), lowNA (b), and highNA (c) population experiments.
A.

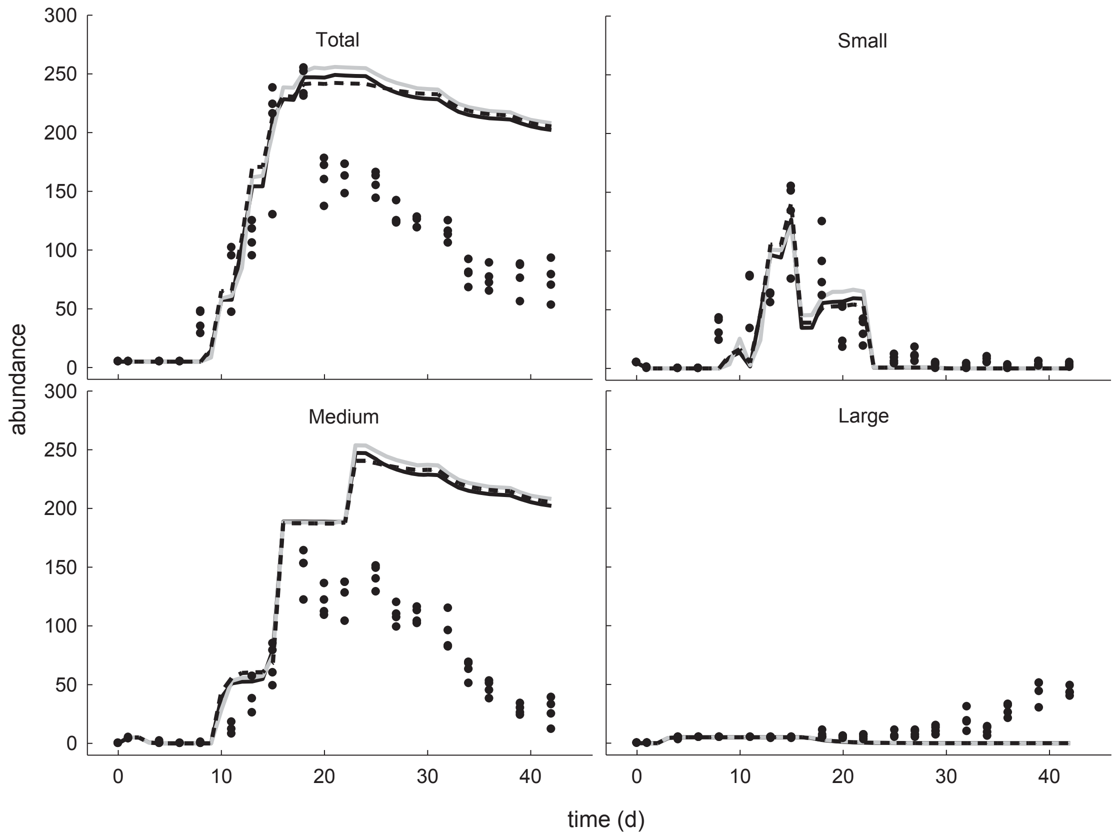

B.

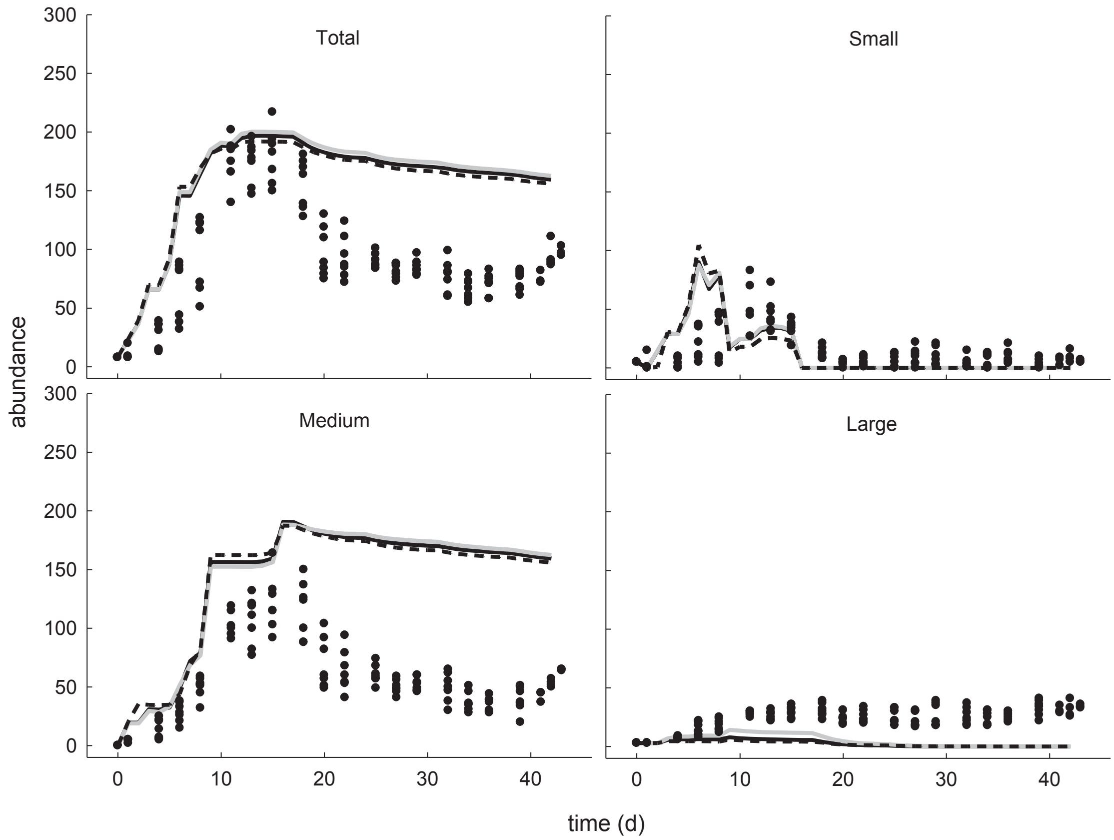
Total
Small
Medium
Large
abundance
time (d)
300
250
200
150
100
50
0
0
10
20
30
40

C.

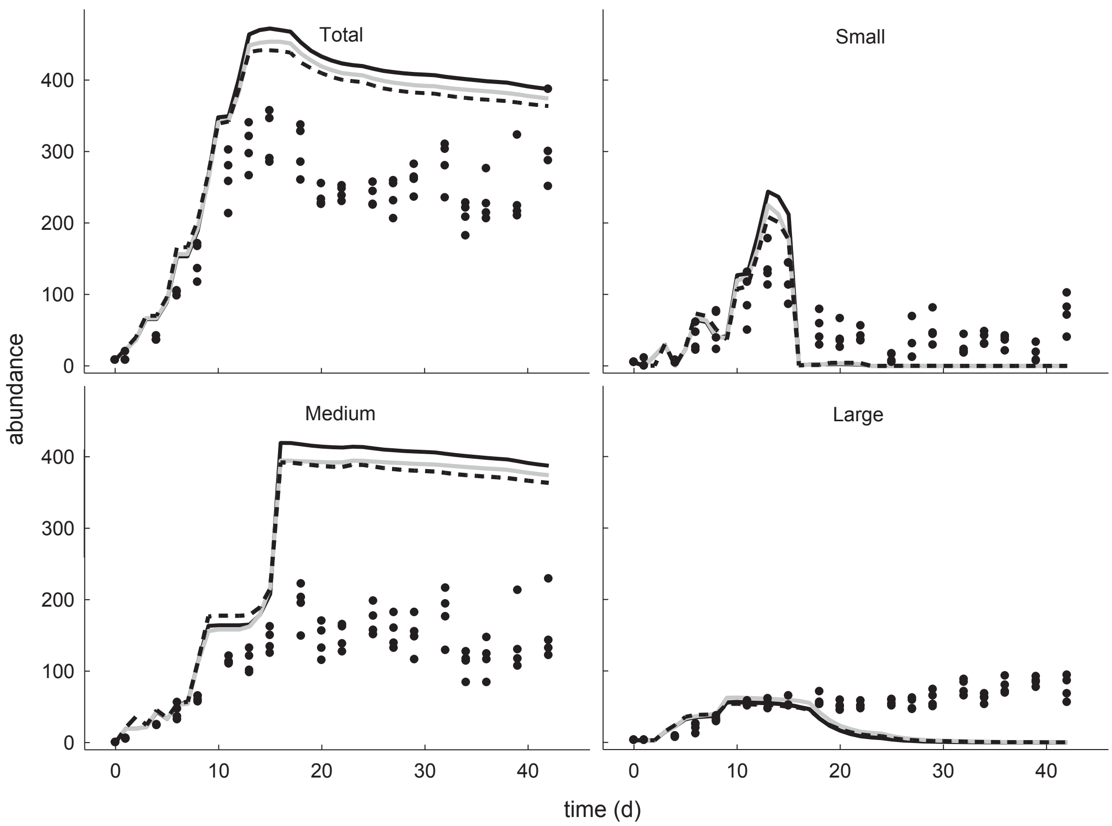

Total
Small
Medium
Large
abundance
time (d)
0
100
200
300
400
0
10
20
30
40

Figure 3. Confidence intervals for DEB parameters using the profile likelihoods method with g fived at a value of 10 (Meeker and Escobar 1995).

A.

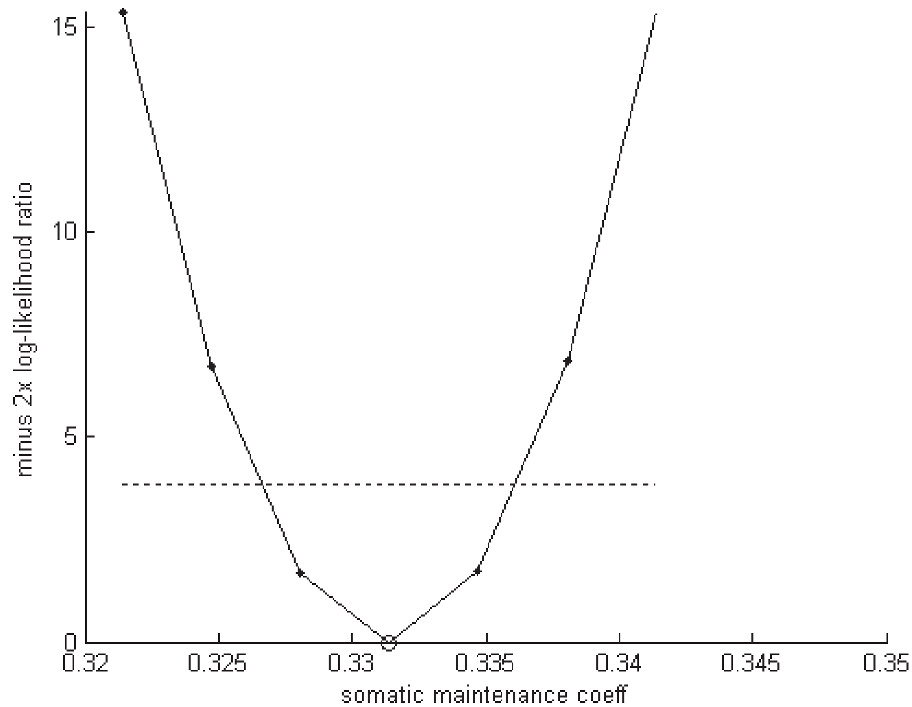

B.

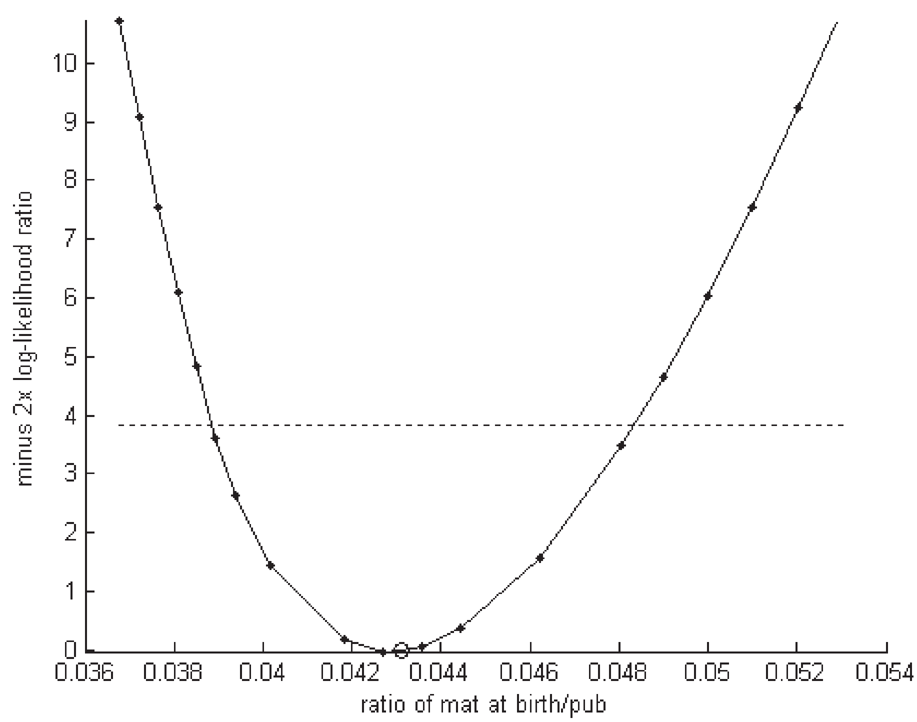

C.

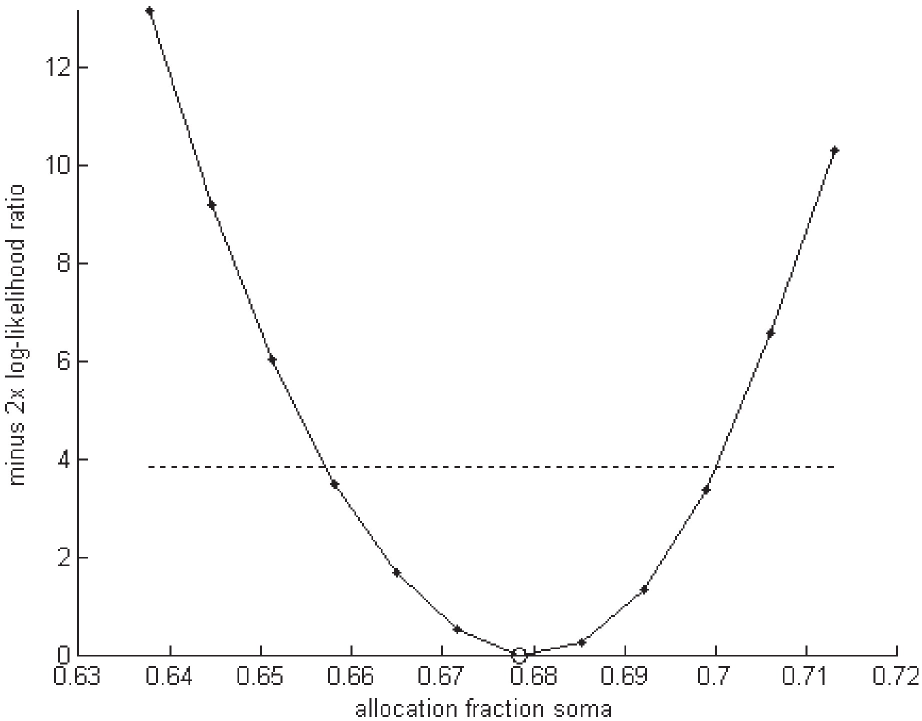

minus 2x log-likelihood ratio
0
2
4
6
8
10
12
0.63
0.64
0.65
0.66
0.67
0.68
0.69
0.7
0.71
0.72
allocation fraction soma

D.

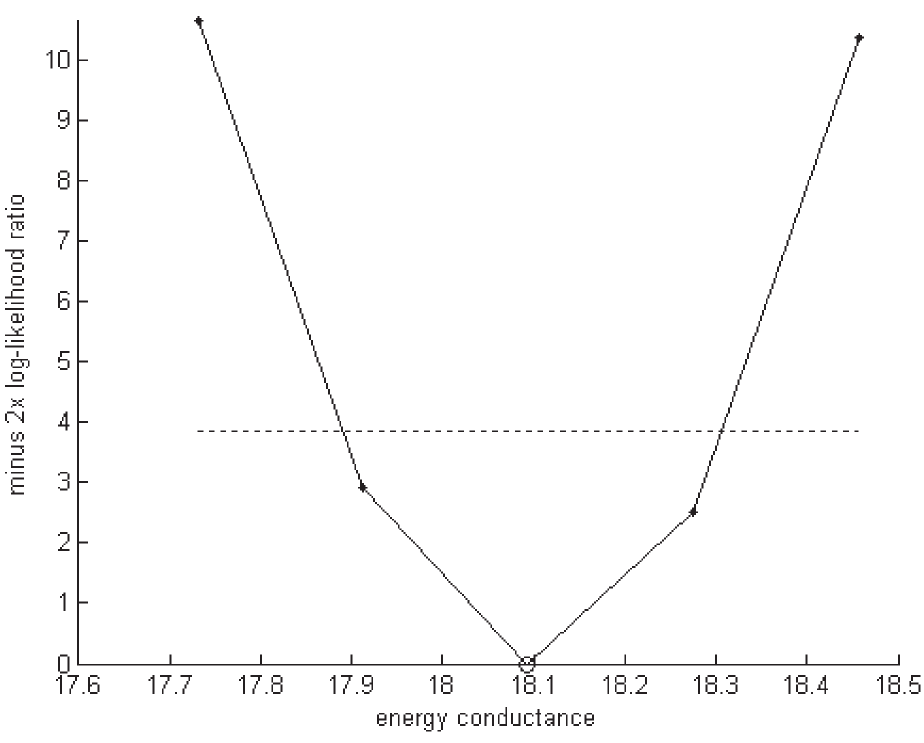

minus 2x log-likelihood ratio
0
1
2
3
4
5
6
7
8
9
10
17.6
17.7
17.8
17.9
18
18.1
18.2
18.3
18.4
18.5
energy conductance

E.

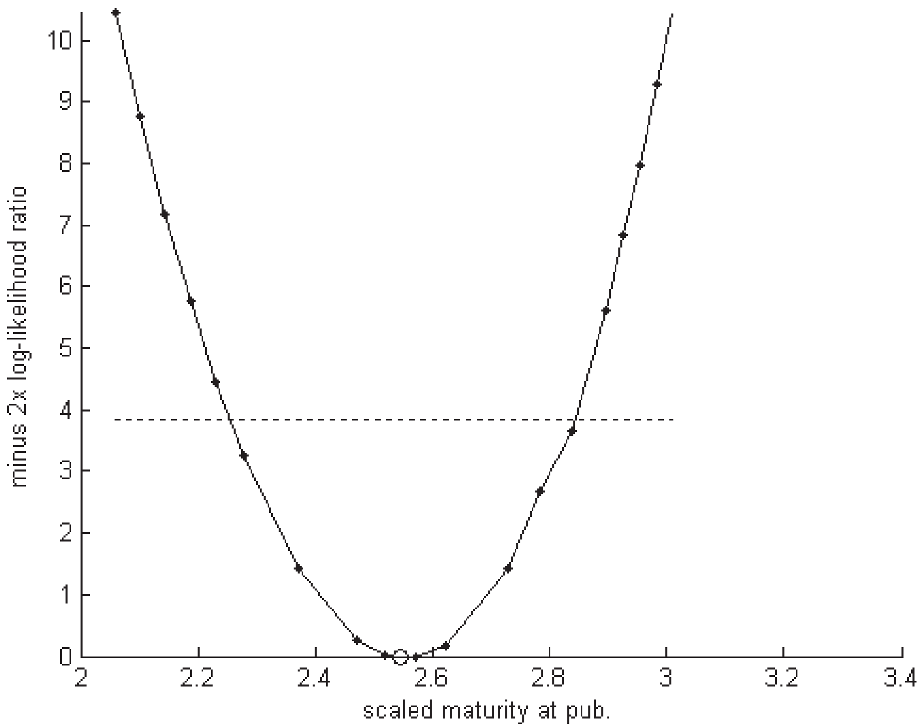

minus 2x log-likelihood ratio
scaled maturity at pub.

F.

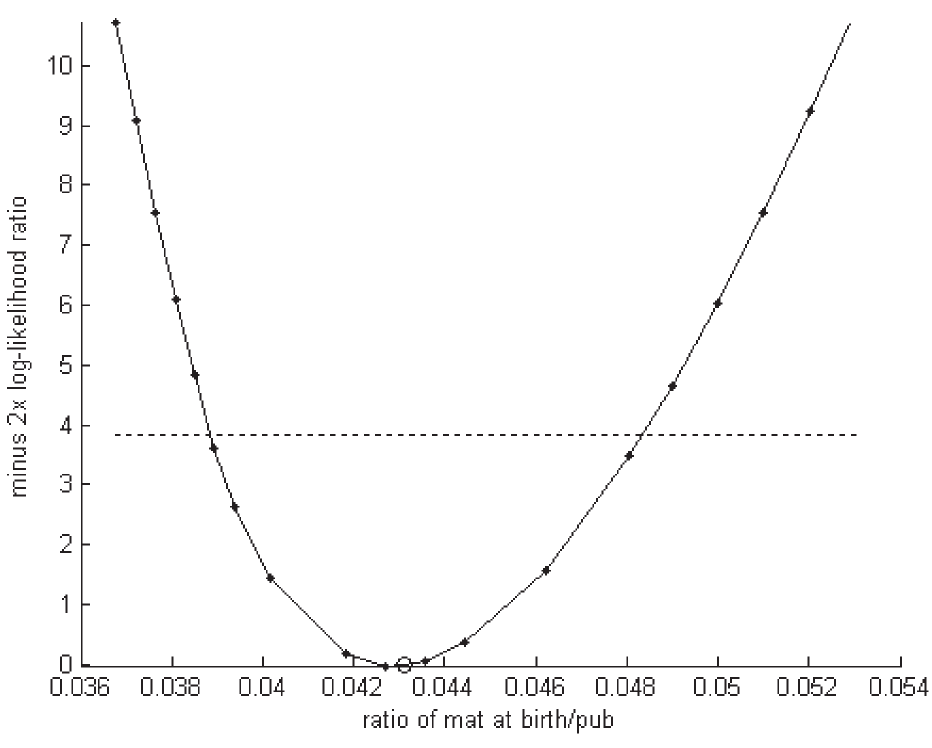

minus 2x log-likelihood ratio
ratio of mat at birth/pub

Figure 4. Confidence interval for Weibull ageing rate, $\dot{k}_W$ (A), and the Gompertz aging rate, $\dot{k}_G$ (B). Note that for use in DEB-IBM we use the aging parameters $\ddot{h}_a$ and s_G, where $\ddot{h}_a = \frac{\dot{k}_W^3}{\dot{k}_m g}$ and $s_G = \frac{\dot{k}_G}{\dot{k}_m g}$.

A.

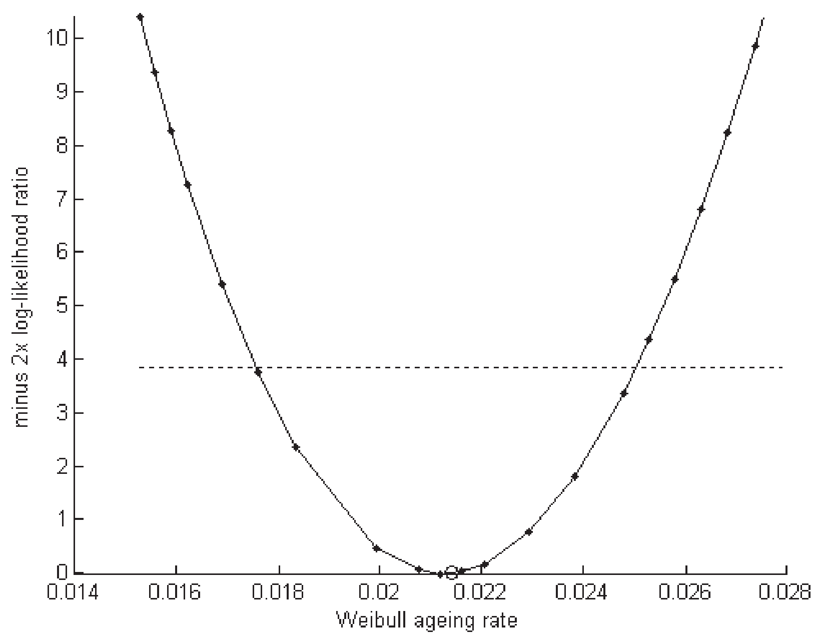

B.

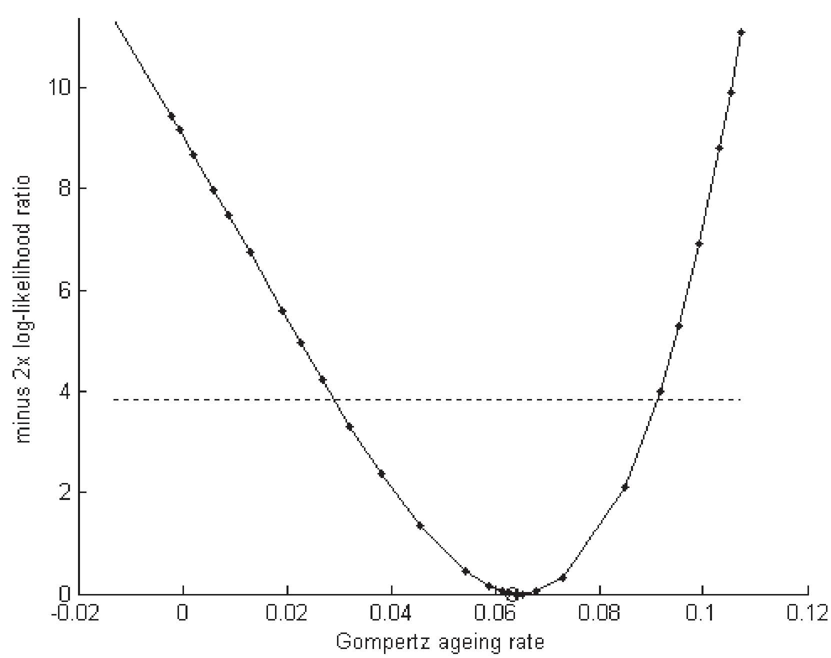

Figure 5. Confidence interval for feeding submodel parameters: the half saturation coefficient (K) and the maximum surface area-specific ingestion rate $\{\dot{J}_{XAm}\}$.

A.

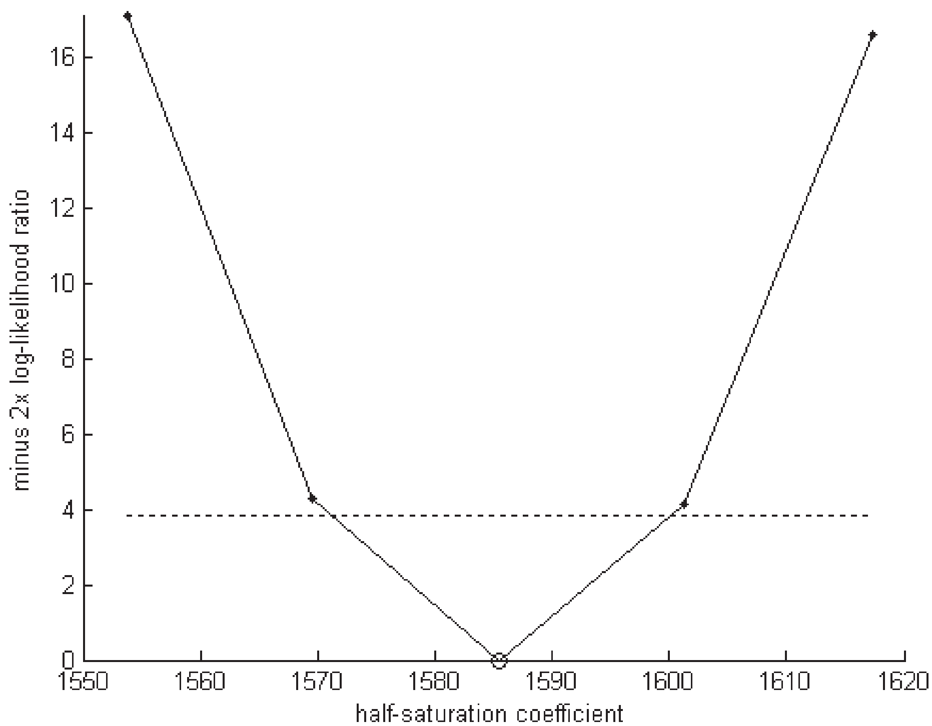

B.

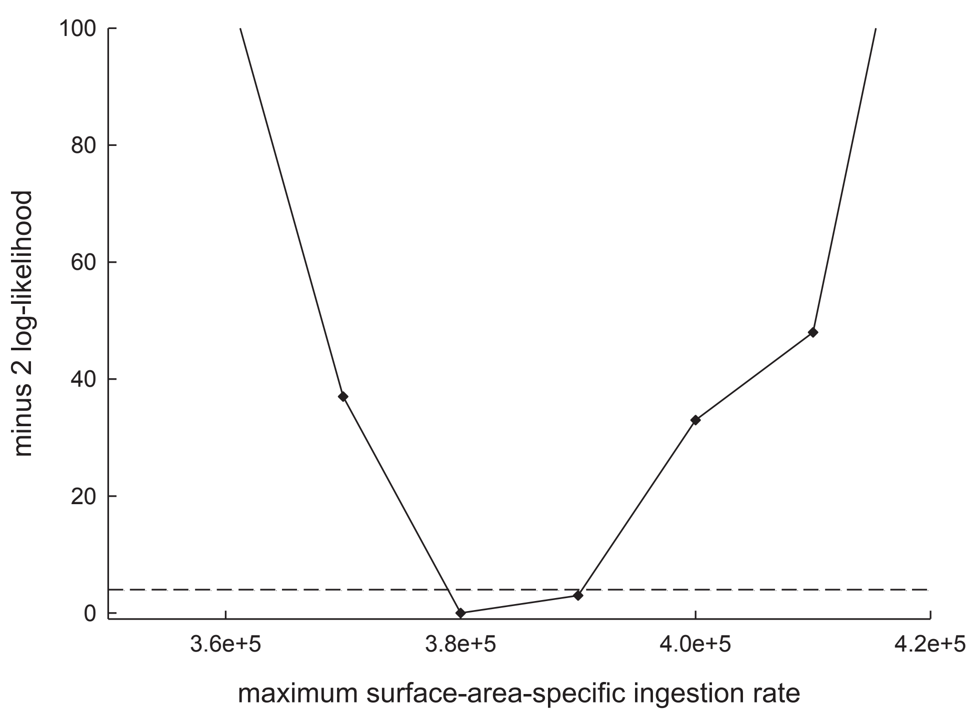

Figure 6. Comparison of DEB-IBM model predictions with the most likely value of $\{\dot{J}_{XAm}\}$ to data from daphnia body size and cumulative reproduction over time (Coors et al.2004). The daphnia experiments and simulations were run under batch food conditions with either 0.05 (a), 0.075 (b), or 0.2 (c) mgC added each day.

A.

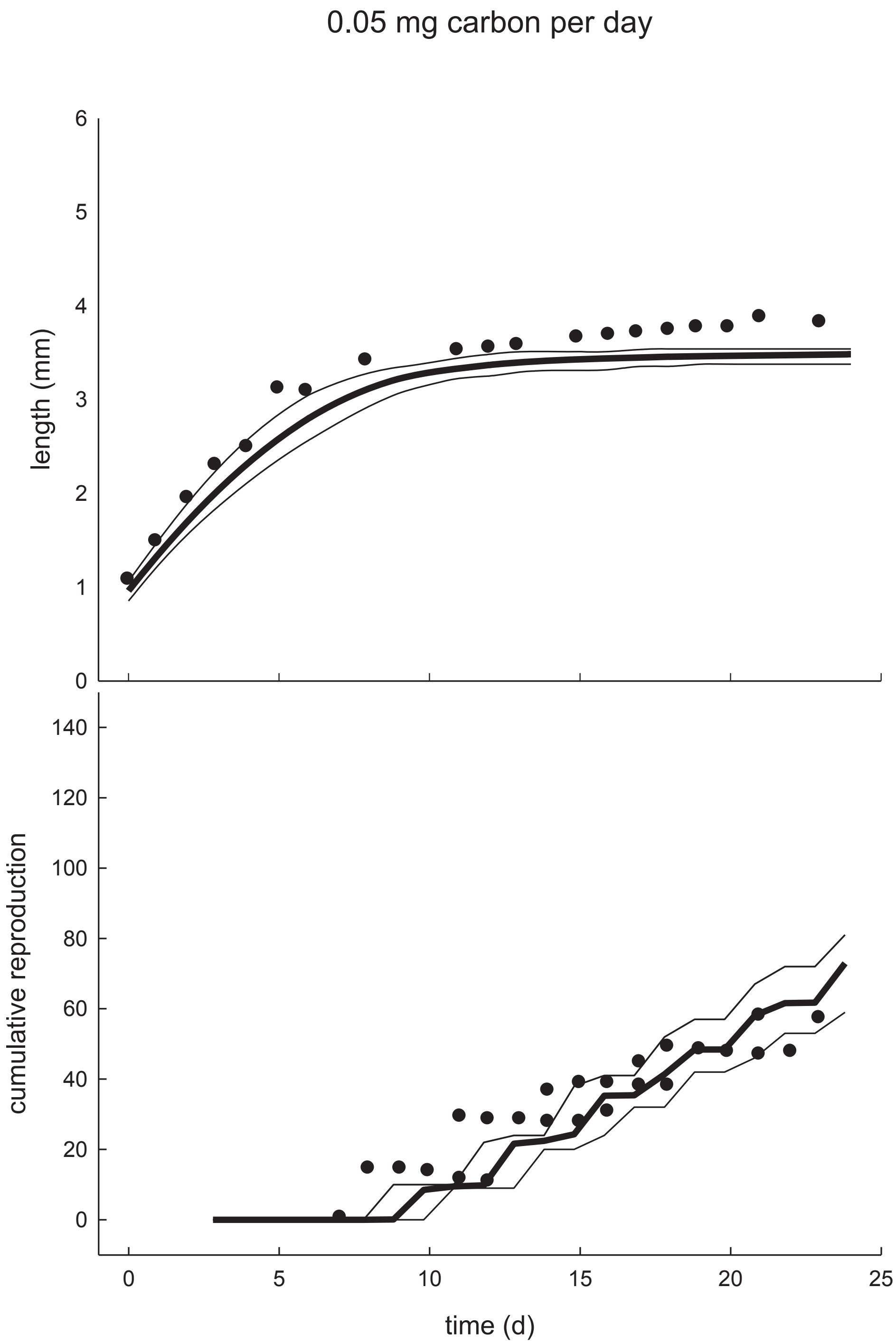

B.

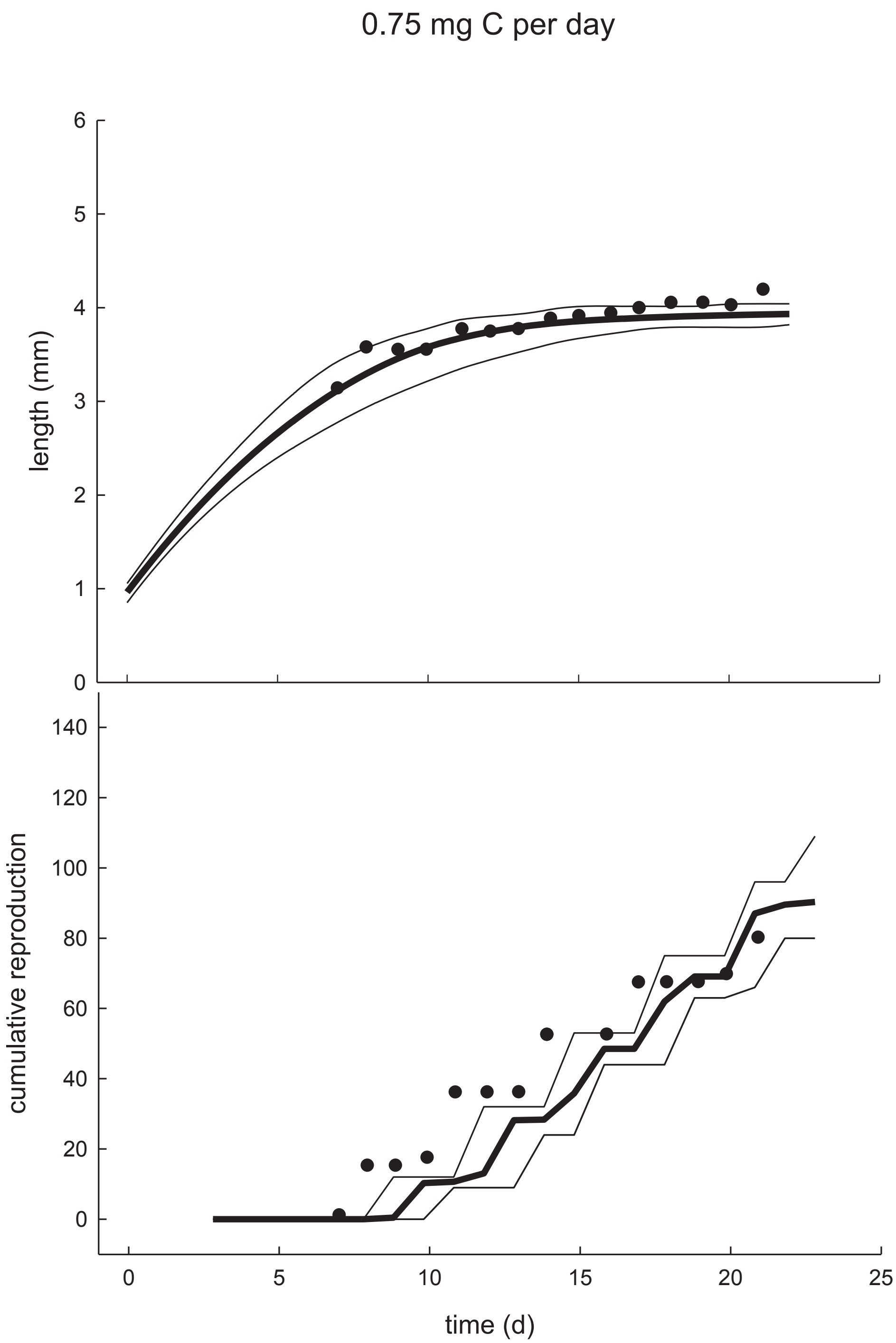
0.75 mg C per day
length (mm)
0
1
2
3
4
5
6
cumulative reproduction
0
20
40
60
80
100
120
140
0
5
10
15
20
25
time (d)

C.

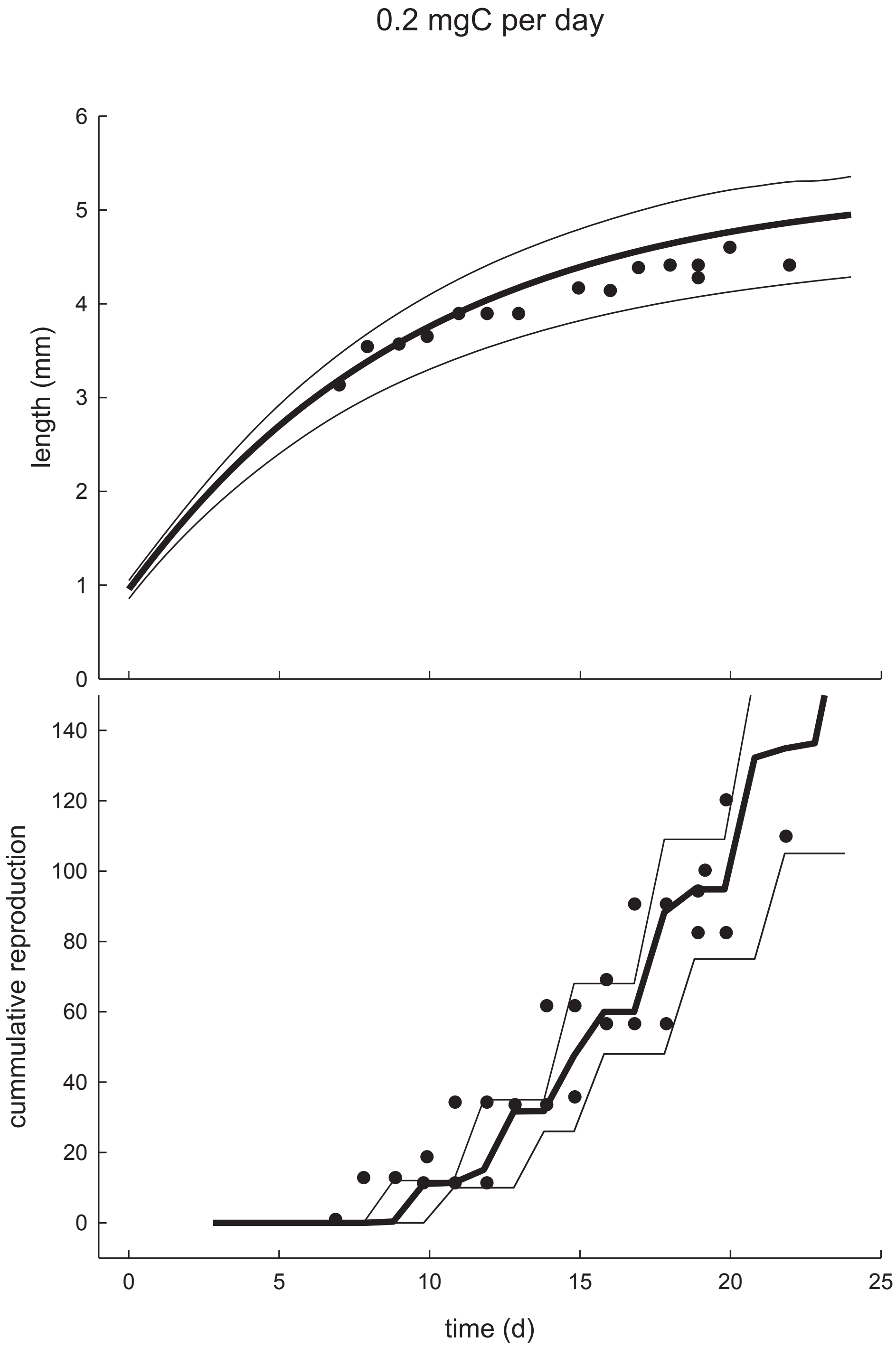

0.2 mgC per day
length (mm)
0
1
2
3
4
5
6
cummulative reproduction
0
20
40
60
80
100
120
140
0
5
10
15
20
25
time (d)

Appendix 2. Model Description (ODD)

Predicting population dynamics from the properties of individuals: a cross-level test of the Dynamic Energy Budget theory

Benjamin Martin[1*], Tjalling Jager[2], Roger Nisbet[3], Thomas G. Preuss[4], Volker Grimm[1,5]

[1] UFZ, Helmholtz Centre for Environmental Research, Dept. of Ecological Modelling, Permoserstrasse 15, 04318 Leipzig, Germany

[2] Vrije Universiteit Amsterdam, FALW/Department of Theoretical Biology De Boelelaan 1085 NL-1081 HV Amsterdam, The Netherlands

[3] University of California, Santa Barbara, Dept. of Ecology, Evolution, and Marine Biology Santa Barbara, CA 93106-9620

[4] RWTH Aachen University, Institute for Environmental Research Worringerweg 1, 52074 Aachen, Germany

[5] University of Potsdam, Institute for Biochemistry and Biology Maulbeerallee 2, 14469 Potsdam, Germany

[*] Corresponding author, email: btmarti25@gmail.com

The model and the ODD model description are adapted from:

Martin, B. T., E. I. Zimmer, V. Grimm, T. Jager. 2012. Dynamic Energy Budget theory meets individual-based modeling: A generic and accessible implementation. Methods in Ecology and Evolution, *in press* DOI: 10.1111/j.2041-210X.2011.00168.x

We recommend reading the article first.

Leipzig – April, 2012

DEB-IBM: Model Description

The model description follows the ODD protocol for describing individual-based models (Grimm et al. 2006, 2010) and is adapted from Martin et al. (2012).

1. Purpose

The purpose of this model is to perform a cross-level test of DEB theory, by parameterizing a DEB model adapted for *Daphnia* at the individual level and comparing the emergent population dynamics to independent experimental data.

2. Entities, state variables, and scales

The model includes two types of entities, *Daphnia* and the environment. Each *Daphnia* is characterized by four primary state variables, henceforth referred to as DEB state variables: structure (L, unit: mm), which determines actual size, feeding rates, and maintenance costs; scaled reserves (U_E, unit: d.mm^2), which serve as an intermediate storage of energy between feeding and mobilization processes; scaled maturity, (U_H unit: d.mm^2), a continuous state variable which regulates transitions between the three development stages (embryo, juvenile, adult) at fixed maturity levels; and finally a scaled reproduction buffer (U_R, unit: d.mm^2) which is converted into eggs during reproductive events. The term "scaled" in reserves, maturity, and buffer refers to the fact that in this "scaled" version of the model the dimension of energy or mass (either as joule or moles of reserve) are scaled out (see Kooijman et al., 2008 and section 2 of the DEB-IBM User Manual from Martin et al. 2012).

In addition to these DEB state variables, intrinsic variation among individuals is created by including a random component in some of the individuals' eight "DEB-IBM parameters". Each individual has a state variable we refer to as a "scatter multiplier" which is a log-normally distributed number, by which four of the standard DEB parameters are multiplied to get the individual-specific set of DEB parameters (see stochasticity section).

Additionally the model includes an ageing submodel based on DEB theory which includes two state variables, damage inducing compounds ($\ddot{q}$), and damage ($\dot{h}$).The aging process is tightly linked to energetics in that the production of damage-inducing compounds is proportional to mobilization (energy utilization). Damage inducing compounds produce damage and thereby affect survival probability. In addition to directly producing damage, damage inducing compound also can proliferate by inducing their own production (see ageing submodel).

The second entity in the model is the environment, which is defined by the state variables food density and temperature. The simulations are designed to replicate the “batch-fed” experiments conducted in Preuss (2009), where a specific amount of food (algal cells) is added on fixed days. Food is depleted from the environment via feeding by the *Daphnia*.

All simulations represent dynamics in a 900 ml vessel, and the model is non-spatial, as we assume food and daphnia are well mixed within the container.

3. Process overview and scheduling

Individuals update their DEB state variables based on a discretized form of the differential equations. At each time step, a set of discrete events may occur. If an organism can no longer pay all maintenance costs (the growth equation becomes negative), individuals cover maintenance costs by burning structure (shrink). If individuals shrink below a specific proportion of their previous maximum body size (crit-mass) they have a high probability of dying (0.35 per day). The second source of mortality is death via ageing. Each timestep individuals have a probability of dying which is proportional to their damage state variable, $\dot{h}$. Finally, mature individuals reproduce at fixed intervals equivalent to the length of a typical molt period for a daphnia (2.8 days). At the reproduction timestep, mature *Daphnia* convert all energy accumulated during the previous molt period to embryos; the number of embryos produced is equal to energy accumulated in the reproduction buffer divided by the cost of producing an embryo (see Reproduction submodel for details).

The following pseudo-code describes the scheduling of events within one timestep of the numerical solution of the model equations (see “go” procedure in NetLogo implementation):

```
For each individual
  [
    Calculate change in reserves
    Calculate change in length
    If mature
      [
        Calculate change in reproduction buffer
      ]
    Else
      [
        Calculate change in maturity
      ]
    Calculate change in ageing acceleration
    Calculate change in hazard
  ]
For the environment
  [
    Calculate food depletion
  ]

For mature individuals
  [
    Update molt-time
    if molt-time >= time-between-molts
      [
        Release offspring created at last molt
        Create embryos from reproduction buffer that will hatch the
        next brood
        Set molt-time 0
        Set reproduction buffer back to 0
      ]
  ]
Update individual state variables
Update environmental state variables
```

4. Design concepts

Basic principles

The model is based on the Dynamic Energy Budget theory (Kooijman 1993, 2000, 2010). An overview of the concepts can be found in Kooijman (2001) or Nisbet et al. (2000). The theory is based on the general principle that the rates of fundamental metabolic processes are proportional to surface area or body volume and a full balance for mass and energy.

Emergence

Traits of the individual and structure and dynamics of the population emerge from the properties of metabolic organization and indirect interactions of individuals via competition for food.

Adaptation

The framework does not include adaptive behavior; in particular, DEB parameters vary among individuals but remain constant over an individual's lifespan. Consequently, the design concepts "objectives", "learning", "prediction", and "sensing" do not apply to this framework.

Interaction

Individuals interact indirectly via competition for food.

Stochasticity

There are three sources of stochasticity in the model. The first source is intra-specific differences in parameter values. We followed the method outlined in Kooijman (1989) where the surface-area-specific maximum assimilation rate of an individual (reffered via index i) is given by multiplying the corresponding species-specific rate $\{\dot{J}_{EAm}\}$ with the individual-specific scatter multiplier SM_i. The "scatter multiplier" is a log-normally distributed random number with a standard-deviation which is user defined. However, since DEB-IBM is based on the scaled, not the standard, DEB model where $\{\dot{J}_{EAm}\}$ is scaled out of the model, $\{\dot{J}_{EAm}\}$ is a "hidden" parameter affecting four other scaled and compound parameters. These interrelationships are described in detail in section 2 of the DEB-IBM User Manual of Martin et al. (2012). For our simulations we used a value of 0.05 for the standard deviation for the scatter multiplier. The second source of stochasticity is that all mortality processes are probabilistic. Finally the last source of stochasticity is in the submodel representing food input. Although in the experiments a fixed amount of cells are added each day, we assume some variation in the actual amount of food added to the experimental vessel by assuming a standard deviation of 10% of the daily food input.

Observation

Over the course of the 43 days of simulation we keep track of both the total *Daphnia* abundance and the abundance of three size classes of *Daphnia*. In the experiments size classes were grouped by filtering the daphnia throw various sized mesh filters. Size classes were calculated based on the diameter of the mesh size multiplied by a factor of 1.25. Previously it has been assumed daphnia pass through the mesh with their smallest side, so that value 1.6 was used which corresponds to the length to width ratio of the clone of *Daphnia* used in the study. We calculated the value 1.25 by comparing the number of *Daphnia* in each size class to a replicate experiment where each daphnia was measured (Agatz et al. 2012) Using a conversion factor of 1.25 provided the greatest agreement between the individually measured data (Agatz et al. 2012) set and the grouped-by-mesh-size-class data set (Preuss 2009). This corresponds to size classes of: small (< 1.1 mm), medium (1.1 – 2.0), and large (> 2.0).

5. Initialization

Simulations are initialized with conditions corresponding to the experimental conditions they are supposed to represent. Our simulation model experiments with two different initial conditions. The first type starts with five new born daphnia (neonates) less than 24 hours old. The second starts with three adults, in addition to five neonates. We mirror these initial conditions for neonates by starting with newly hatched *Daphnia*, and simulating a random amount of development time between 0 and 24 hrs, selected from a uniform distribution. For adults we simulated growth at *ad libidum* conditions until each was 4 mm in length, as those used in the experiments. Moreover, as in the experimental setup, each individual was bearing eggs at different levels of development, one nearly complete (0.1 days from hatching), one with eggs midway through development (1.55 days from hatching), and one eggs just beginning development (2.65 days from hatching). When food level was given as carbon content, we recalculated in cell ml^{-1} assuming that *Desmodesmus subspicatus* has an average carbon content of 1.95 x 10^{-8} mgCcell^{-1} (Sokull-Kluettgen 1998; Preuss et al. 2009).

6. Input data

The framework does not include input data representing external driving processes.

7. Submodels

Calculate change in reserve

The change in energy reserves U_E of an individual in a time step is determined by the difference in scaled assimilation S_A and mobilization S_C fluxes.

$$\frac{d}{dt}U_E = (S_A - S_C)$$

where

$$S_A = fL^2$$

and

$$S_C = L^2 \frac{ge}{g+e}\left(1 + \frac{L\dot{k}_M}{\dot{v}}\right)$$

where

$$e = \dot{v}\frac{U_E}{L^3}$$

and

$$f = \frac{X}{K+X} \text{ for } U_H > U_H^b$$

Because embryos do not feed exogenously

when $U_H < U_H^b \quad f = 0$

the assimilation flux will be zero and the change in reserves is reduced to:

$$\frac{d}{dt}U_E = -S_C$$

Rationale:

DEB theory includes a state variable "reserve" which acts as an intermediate between the feeding and mobilization process. Reserves allow for metabolic memory, i.e. the metabolic behavior of individuals is not solely dependent on the current food availability, but rather the "recent" feeding history of an individual. For example animals can continue to grow for a short period of time when food has been removed from their environment.

Calculate change in maturity

Individuals begin with a maturity level U_H of 0, which increases each time step according to the differential equation:

$$\frac{d}{dt}U_H = (1-\kappa)S_C - \dot{k}_j U_H \quad \text{when} \quad U_H < U_H^p$$

else

$$\frac{d}{dt}U_H = 0$$

Transitions between development stages occur at set values of maturity. An embryo which feeds exclusively on reserves becomes an exogenously feeding juvenile when $U_H > U_H^b$ and a reproducing adult when $U_H > U_H^p$. Once puberty is reached, maturity is fixed and energy previously directed towards maturity is now allocated to the reproduction buffer. Before *Daphnia* reach puberty, if mobilized energy is not enough to pay maturity maintenance costs, the maturity flux can become negative, and animals decrease in maturity.

Rationale:

Immature individuals divert mobilized energy from reserves between competing functions of growth and development, with the proportion 1-κ of mobilized reserves allocated to development. Individuals first pay maintenance costs associated with maintaining their current level of maturity (the maturity maintenance rate coefficient, $\dot{k}_J$, multiplied by the current level of maturity, U_H) from the mobilized reserves directed toward development from the mobilized reserves [$(1-\kappa)S_C$]. The remainder represents the increase in development during a timestep.

Calculate change in reproduction buffer

When an individual has reached puberty, energy from the maturity flux is diverted into a reproduction buffer, U_R.

$$\frac{d}{dt}U_R = (1-\kappa)S_C - \dot{k}_J U_H^p \text{ for } U_H > U_H^p$$

else

$$\frac{d}{dt}U_R = 0$$

If mobilized energy is not enough to pay maturity maintenance costs, the reproduction buffer flux becomes negative to pay maturity maintenance costs. If the reproduction buffer flux is negative, but there is no energy remaining in the reproduction buffer, maturity maintenance is not paid (U_R cannot be < 0).

Rationale:

This submodel is basically the same as for the delta maturity calculation, but is calculated only for mature individuals, whose maturity does not increase. The energy that accumulates in the reproduction buffer in a given time step is the difference between mobilized energy allocated towards reproduction and the fixed maturity maintenance costs.

Calculate change in length

During a timestep energy needed for somatic maintenance costs are paid from mobilized energy allocated for soma. The remainder is converted from reserve to structural length. Under non-starvation conditions:

$$\frac{d}{dt}L = \frac{1}{3}\left(\frac{\dot{v}}{gL^2}S_C - \dot{k}_M L\right)$$

The parameter κ, which determines the fraction of mobilized energy directed to the soma is not explicit in this formula, however, κ, is in the compound parameter *g* (see section 2.4 in the User Manual of Martin et al. (2012) for a discussion of compound parameters).

If mobilized energy allocated towards somatic growth and maintenance is insufficient to pay somatic maintenance costs, growth becomes negative. Essentially the *Daphnia* pay maintenance costs by “burning” their structure. When an individual shrinks below 40% of its previous maximum mass, the individual then has a mortality rate of .35 d^{-1}.

Rationale:

When mobilized reserves allocated to the soma are insufficient to pay somatic maintenance costs, animals may respond in many ways, which can be represented in DEB, for example by shrinking in structure (see Kooijman 2010 for discussion of starvation strategies). Our implementation of the starvation model assumes that daphnia get 100% of the energy invested in growth back to pay maintenance costs when shrinking.

Reproduction submodel

DEB makes no general assumptions about the reproduction buffer handling rules, and these must therefore be defined for each species. *Daphnia* release clutches of embryos during the molt, using energy accumulated over the intermolt period. These embryos develop in the brood chamber over the next intermolt period, and are released during the next molt, at which time they begin feeding exogenously. Below we describe how this process is replicated mathematically.

At the timestep where *Daphnia* reach maturity ($U_H = U_H^p$), they set a state variable “molt-time” to 0. In each subsequent timestep the state “molt-time” ticks up by the amount of time transpired until it reaches the parameter “time-between-molts”. This was set to 2.8 days, which approximates the molt length of daphnia in 20C. When molt-time >= time-between-molts, the *Daphnia* convert energy accumulated in the reproduction-buffer (U_R) into embryos. The number of embryos produced is given by:

$$N = \left\lfloor \frac{U_R \kappa_R}{U_{Embryo}} \right\rfloor$$

Here κ_R represents the conversion efficiency of the reproduction buffer to the reserves of the embryo which is assumed to be high as both in DEB theory are assumed to have the same composition. The cost of producing one embryo, U_E^0, is the amount of energy needed to create one offspring that will reach the maturity for birth threshold ($U_H = U_H^b$) with a reserve density, *e*, equal to 1. This value is dependent on the DEB parameters of a species and is calculated numerically using the bisection method during the setup up procedure. The initial bounds for the bisection method were set to 0 and an unrealistically high number to ensure the true value was contained within the initial bounds. Values of U_E^0 were tested by simulating the embryonic period following the mass balance equations of DEB theory. In DEB theory embryos start out as nearly all reserves, and a very small amount of structure. During the embryonic period, embryos mobilize reserves to grow and gain maturity. The selection criteria for the value of U_E^0 was that embryos was within 5% of a reserve density e = 1 when the maturity threshold for birth was surpassed. With the parameter values used for daphnia in our simulations this corresponded with a length at birth = 0.851 mm. This later value falls well within the range of observed hatching sizes of daphnia magna.

In the simulations, after the calibration of the U_E^0 value we do not simulate the embryonic period. Rather we use the U_E^0 value to determine how many offspring are produce, then in the subsequent molt offspring are created equal to the number of embryos produced in the previous molt, and their state variables are set to the values determined in the calibration period (L_b= 0.851, $e = 1$, $U_H = U_H^b$).

Prey dynamics submodel

Prey dynamics were modeled to replicate the experimental design. In the experiments food was added at the nominal amount Monday-Thursday and on Friday given triple to normal food amount, with no feeding on Saturday or Sunday. We matched this pattern by updating the food state variable (*X*) the appropriate amount. Food is depleted from the environment via feeding of daphnia. The sum of all feeding by *Daphnia* is given as:

$$P_X = \sum_i f L_i^2 \{\dot{J}_{XAm}\}_i$$

Ageing submodel

The basic premise of the DEB aging submodel is that damage inducing compounds are created at a rate proportional to reserve mobilization. Damage inducing compounds induce more damage inducing compounds also at a rate proportional to mobilization. The hazard rate for mortality due to ageing of an individual is proportional to density of the accumulated damage in the body. Additionally, the concentration of both damage inducing compounds and damage are assumed to be diluted via growth. The ageing submodel includes two new parameters: the Weibull ageing acceleration parameter, $\ddot{h}_a$, and the Gompertz stress coefficient, s_G. To reduce the total number of parameters, the equations for damage-inducing compounds, damage and hazard rate are scaled and combined to two ODE's, for "scaled acceleration" ($\ddot{q}$) and hazard rate ($\dot{h}$):

$$\frac{d}{dt}\ddot{q} = (\ddot{q}\frac{L^3}{L_m^3}s_G + \ddot{h}_a)e(\frac{\dot{v}}{L} - \dot{r}) - \dot{r}\ddot{q} \text{ where } \dot{r} = \frac{3}{L}\frac{d}{dt}L$$

$$\frac{d}{dt}\dot{h} = \ddot{q} - \dot{r}\dot{h}$$

Rationale:

In our framework ageing processes are linked tightly to energetics as the production of damage inducing compounds are proportional to mobilization. One interpretation of this assumption is that the production of free radicals or other reactive oxygen species is proportional to the use of dioxygen in metabolic processes. The inclusion of energetics in the ageing process allows differences in ageing of animals in feeding conditions or physiological phenotypes to be explained without altering ageing parameters.

Alternative models of starvation and recovery

In addition to the standard model we tested alternative models of starvation and recovery. These modifications are explained in the main text.

Literature Cited

Agatz A., Hammers-Wirtz M., Gabsi F., Ratte H.T., Brown C.D., Preuss T.G. (2012) Promoting effects on reproduction increase population vulnerability of *Daphnia magna.*; *Environmental Toxicology and Chemistry in press*

Chipps, S. R. and D. H. Wahl. (2008) Bioenergetics Modeling in the 21st Century: Reviewing New Insights and Revisiting Old Constraints. *Transactions of the American Fisheries Society*, **137**, 298-313.

Grimm, V., Berger, U., Bastiansen, F., Eliassen, S., Ginot, V., Giske, J., Goss-Custard, J., Grand, T., Heinz, S., Huse, G., Huth, A., Jepsen, J. U., Jørgensen, C., Mooij, W. M., Müller, B., Pe'er, G., Piou, C., Railsback, S. F., Robbins, A. M., Robbins, M. M., Rossmanith, E., Rüger, N., Strand, E., Souissi, S., Stillman, R. A., Vabø, R., Visser, U., and D. L. DeAngelis. (2006) A standard protocol for describing individual-based and agent-based models. *Ecological Modelling*, **198**, 115-126.

Grimm, V., Berger, U., DeAngelis, D.L., Polhill, G., Giske, J., and S. F. Railsback. (2010) The ODD protocol: a review and first update. *Ecological Modelling*, **221**, 2760-2768.

Kooijman, S. A. L. M., N. v. d. Hoeven and D. C. v. d. Werf. (1989) Population consequences of a physiological model for individuals. *Funcional Ecology*, **3**, 325-336, 1989.

Kooijman, S. A. L. M. (1993) *Dynamic energy budgets in biological systems. Theory and applications in ecotoxicology*. Cambridge University Press.

Kooijman, S. A. L. M. (2000) *Dynamic Energy and Mass Budgets in biological systems.* Cambridge University Press.

Kooijman, S. A. L. M. (2001) Quantitative aspects of metabolic organization; a discussion of concepts. *Philisophical Transactions of the Royal Society B*., **356**, 331-349.

Kooijman, S. A. L. M., T. Sousa, L. Pecquerie, J. Van der Meer and T. Jager. (2008) From food-dependent statistics to metabolic parameters, a practical guide to the use of Dynamic Energy Budget theory. *Biological Reviews*, **83**, 533-552.

Kooijman, S. A. L. M. (2010) *Dynamic Energy Budget theory for metabolic organisation*. Cambridge University Press.

Nisbet, R. M., E. B. Muller, K. Lika, and S. A. L. M. Kooijman. (2000) From molecules to ecosystems through Dynamic Energy Budget models. *Journal of Animal Ecology*, **69**, 913-926.

Martin, B. T., E. I. Zimmer, V. Grimm, T. Jager. 2012. Dynamic Energy Budget theory meets individual-based modeling: A generic and accessible implementation. *Methods in Ecology and Evolution*, *in press*

Appendix 3. Supplementary figures.

Figure 1. Comparison of data and DEB-IBM predictions at the population level for the lowNA (A) and highNA (B) experiments. Simulations with DEB-IBM replicated the experimental conditions. Figures show the mean (think black line) and max and min (dashed grey lines) of 100 simulations.

A.

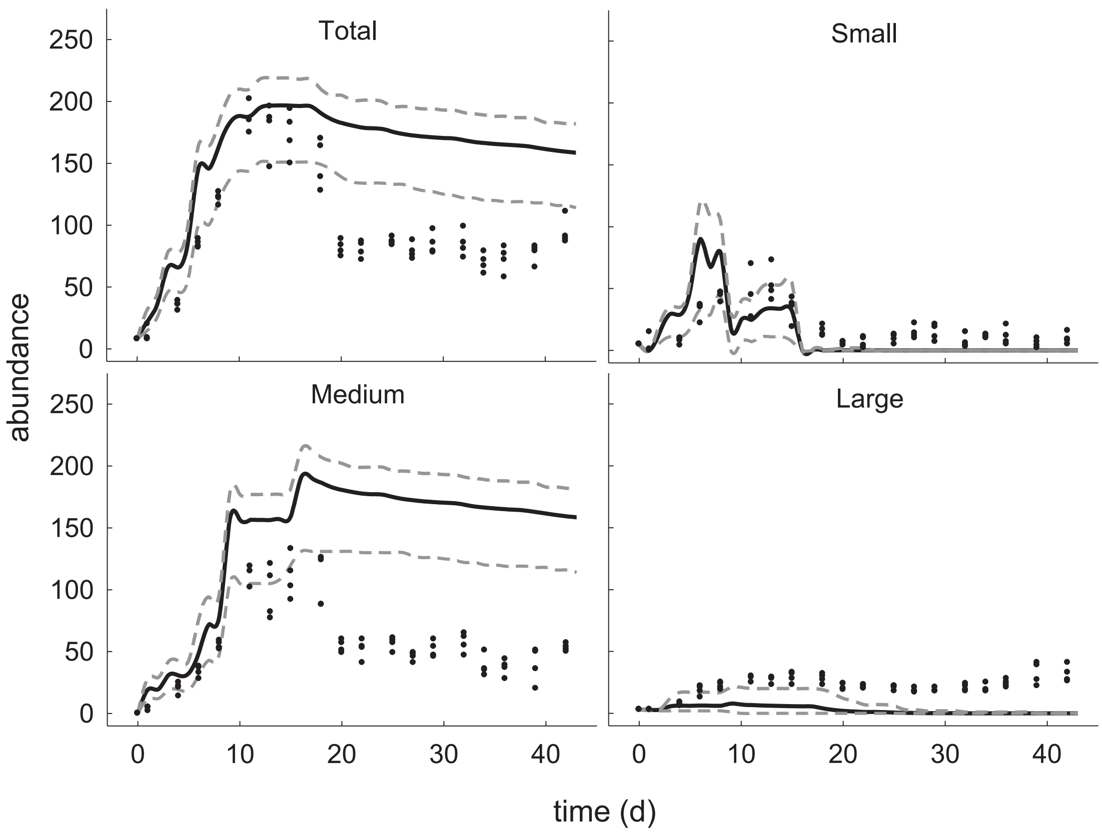

B.

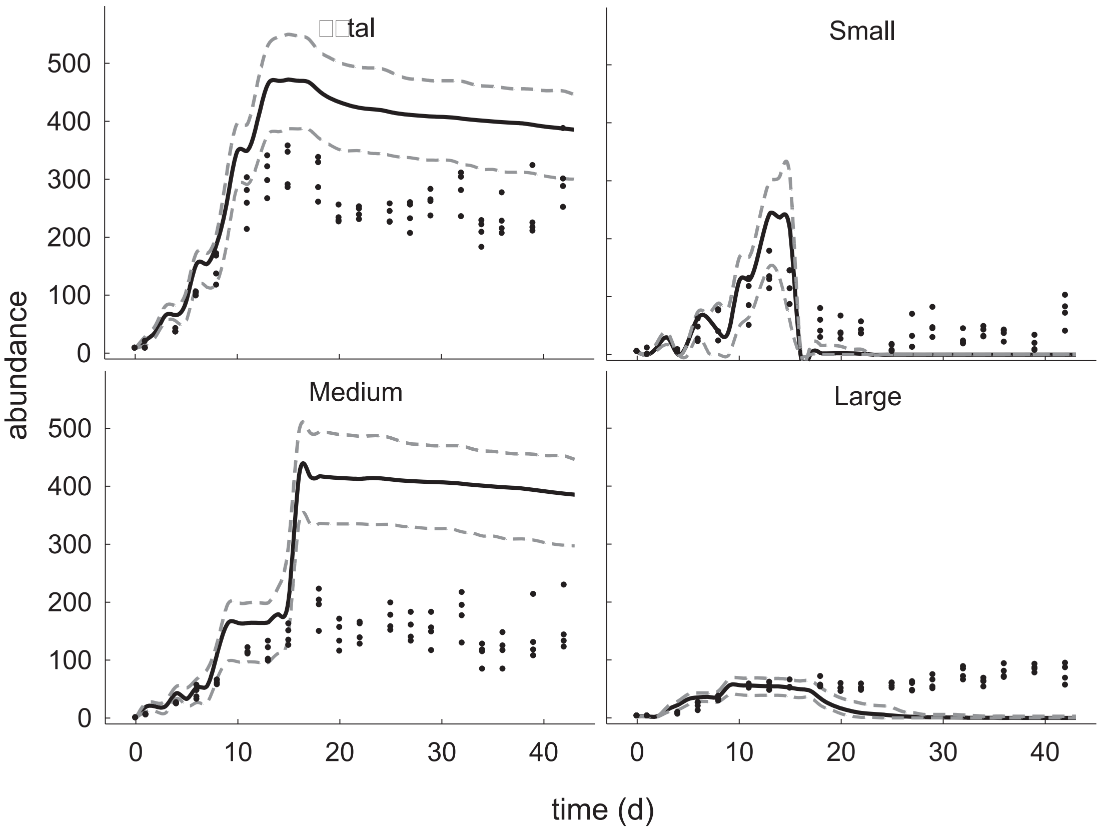

tal
Small
Medium
Large
abundance
time (d)
0
100
200
300
400
500
0
10
20
30
40

Figure 2. Comparison of the performance of three starvation submodels with data from the lowN (A) and lowNA (B) experiments. In each of the three models, a 1 parameter food-dependent mortality submodel, was applied, but models differed in that it was either applied only to juveniles (black solid), only adults (black dashed), or all *Daphnia* (grey solid).

A.

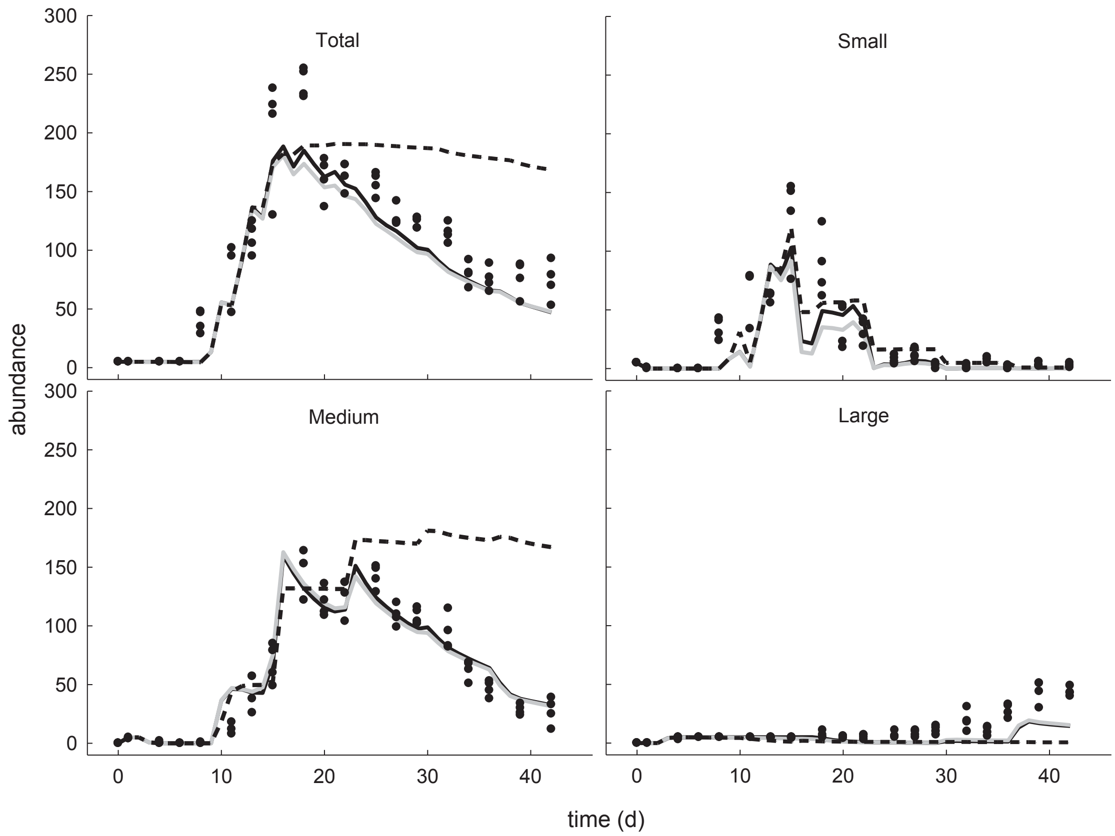

B.

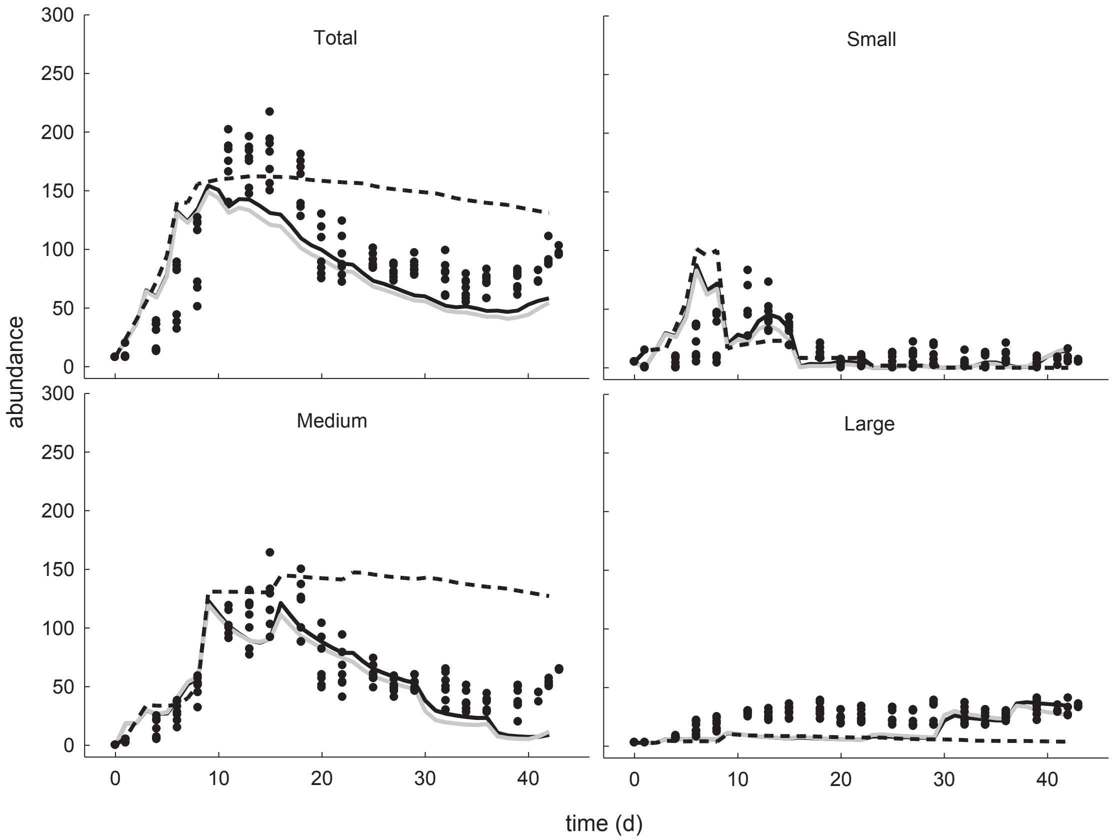

Total
Small
Medium
Large
abundance
time (d)
300
250
200
150
100
50
0
0
10
20
30
40

Figure 3. Comparison of starvation-recovery assumptions at the high food population level for the lowN (A) and lowNA (B) experiments. The grey line show the average of 100 model simulations when individuals feed at a rate proportional to their current length, while the black line represents the average of 100 model simulations when individuals feed at a rate proportional to their maximum length attained.

A.

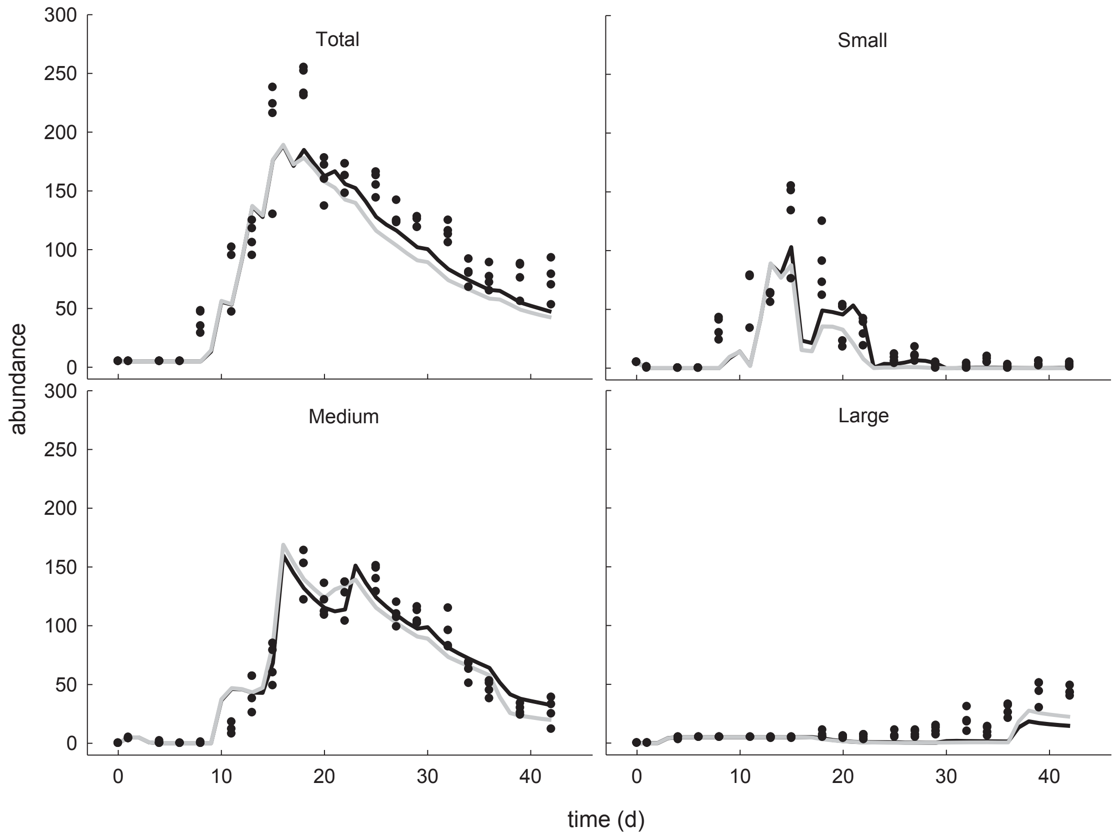

B.

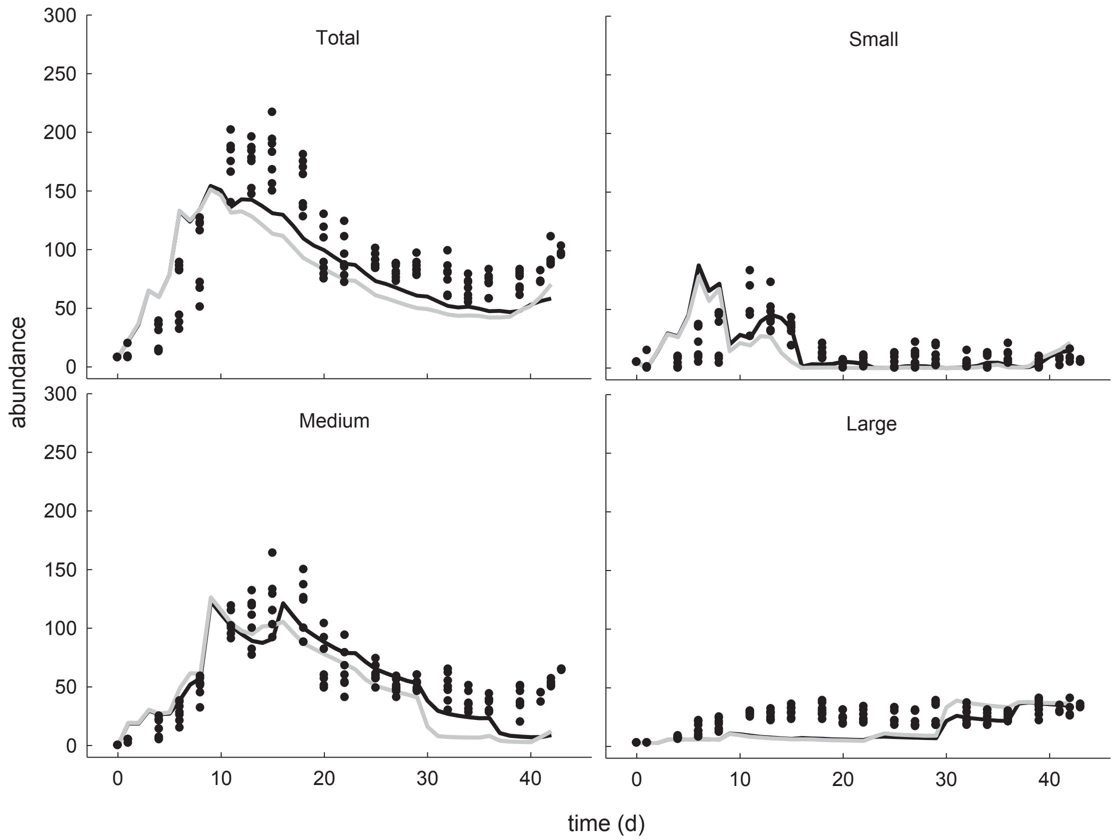

Total
Small
Medium
Large
abundance
300
250
200
150
100
50
0
0
10
20
30
40
time (d)

Other (Video, Excel, large data files)
Click here to download Other (Video, Excel, large data files): DEB_DAPH v1.nlogo